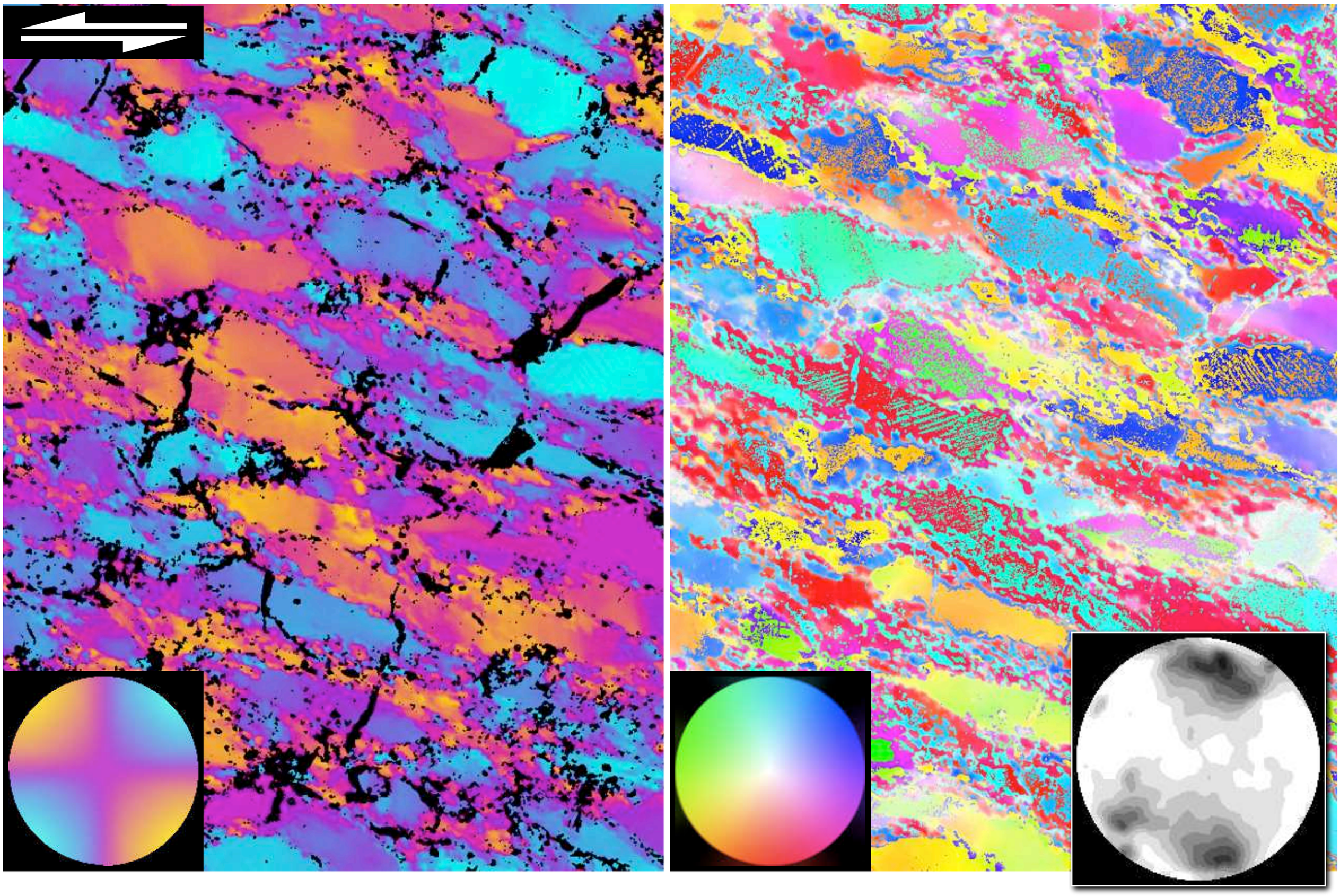

Figure 21.1
Interference color and crystal orientation.
Micrograph of deformed quartzite (left-lateral shear, experiment by Jan Tullis):
(a) as seen in the microscope with crossed polarizers and wave plate inserted;
(b) c-axis orientation image (COI) of (a); corresponding c-axis pole figure in lower right.
The conoscopic image (lower left in (a)) and the color look-up table (CLUT, lower left in (b)) indicate the orientation of the c-axis. Note that conoscopic images (of uni-axial minerals) can be used as look-up table for c-axis orientation.

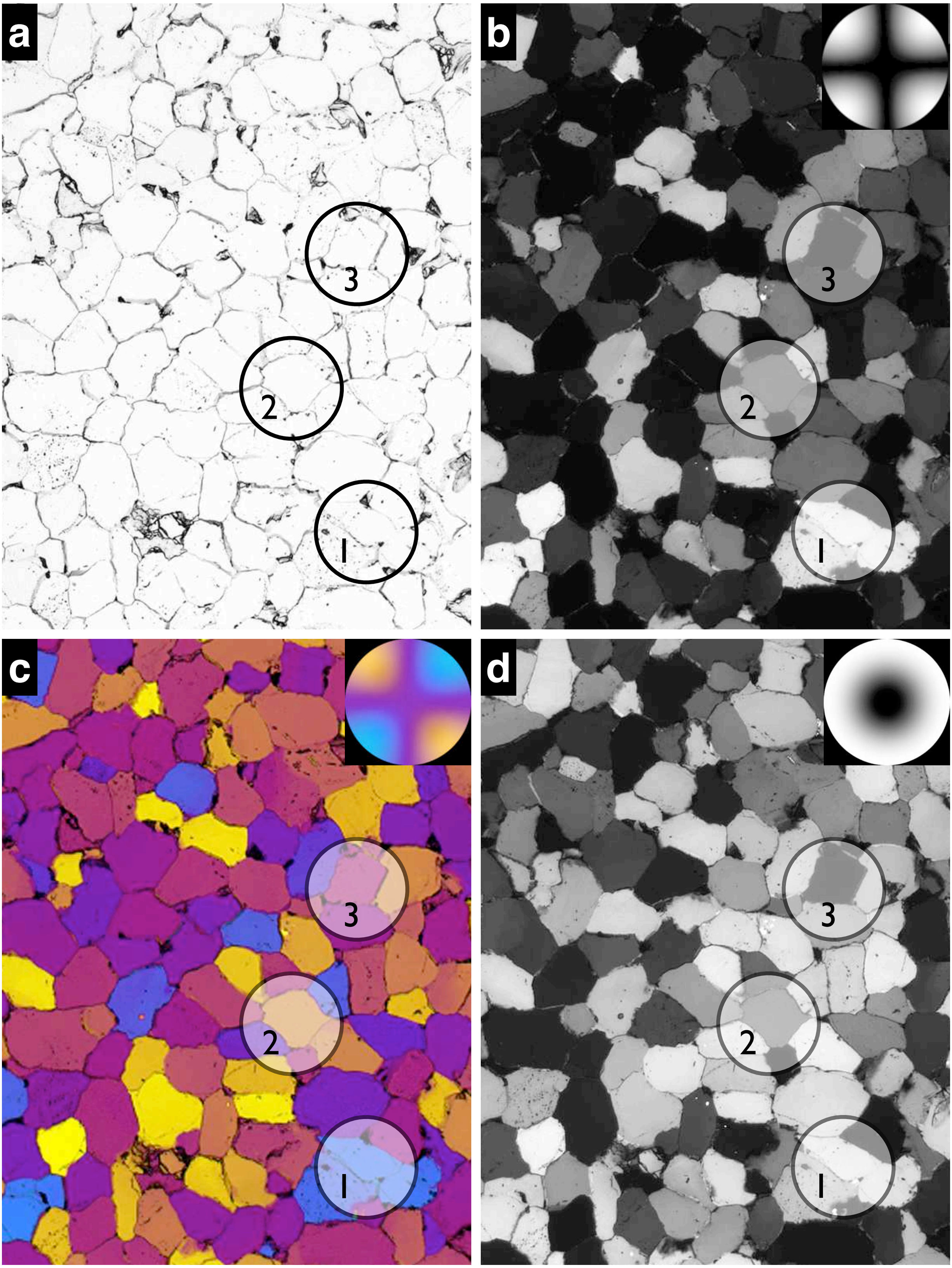

Figure 21.2
Thin sections in the polarization microscope. (a) Thin section of quartzite in plane light; (b) same as (a) crossed polarizers (horizontal and vertical vibration direction); the conoscopic (upper right) shows that quartz is uniaxial; (c) same as (b) with the lambda plate (wave plate) inserted at 45°; on the right, the conoscopic image shows that quartz is optically positive (BURP: Blue Upper Right Positive); (d) circular polarization (= crossed polarizers with two quarter-wave plates inserted at 45° between thin section and upper and lower polarizers); look-up table in upper right indicates the c-axes at low inclinations with respect to to the microscope axis, i.e., normal to the thin section, are dark, those in the plane of the section are bright. Three grains are highlighted (see Figure 21.3).

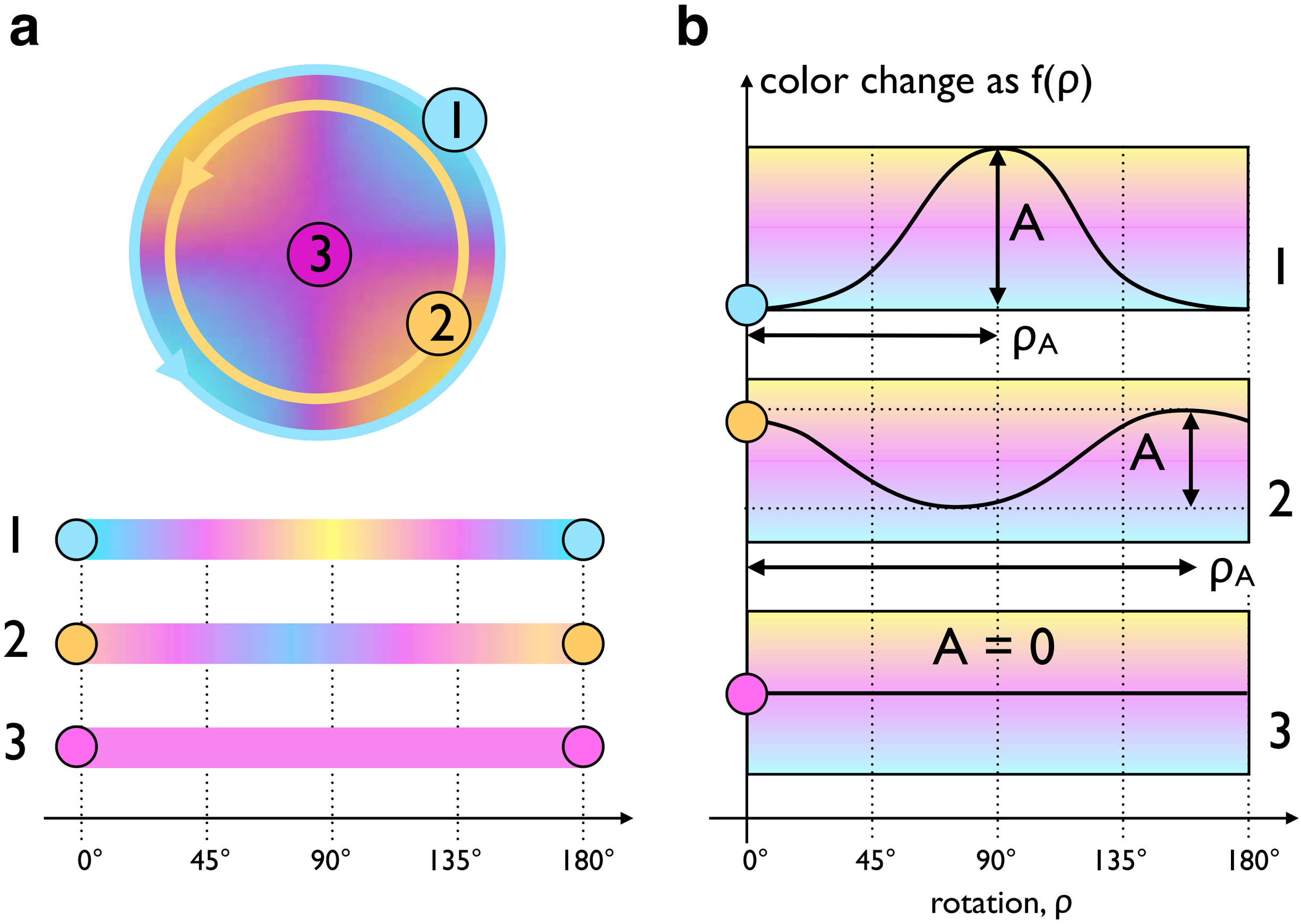

Figure 21.3
Color signal of rotating axes.
Rotating the microscope table causes the c-axes to travel in cones about the microscope axis (i.e., in small circles about the center of the conoscopic image); trajectories of grains in Figure 21.2.
(a) Conoscopic image showing starting positions and trajectories of three grains (1, 2, 3 in Figure 21.2); color changes as function of rotation shown below;
(b) 'color change' function is characterized by amplitude, A, and phase angle, ρ_A.
The larger A, the larger the inclination: if $A = A_{max}$, $\theta = 90°$ (case 1), if $A = 0$ (case 3), $\theta = 0°$. The azimuth of an axis is 45° away from the phase angle, ρ_A; for grain 1, $\rho_A = 90°$, => $\varphi = 45°$; for grain 2, $\rho_A = 165°$, => $\varphi = 120°$.

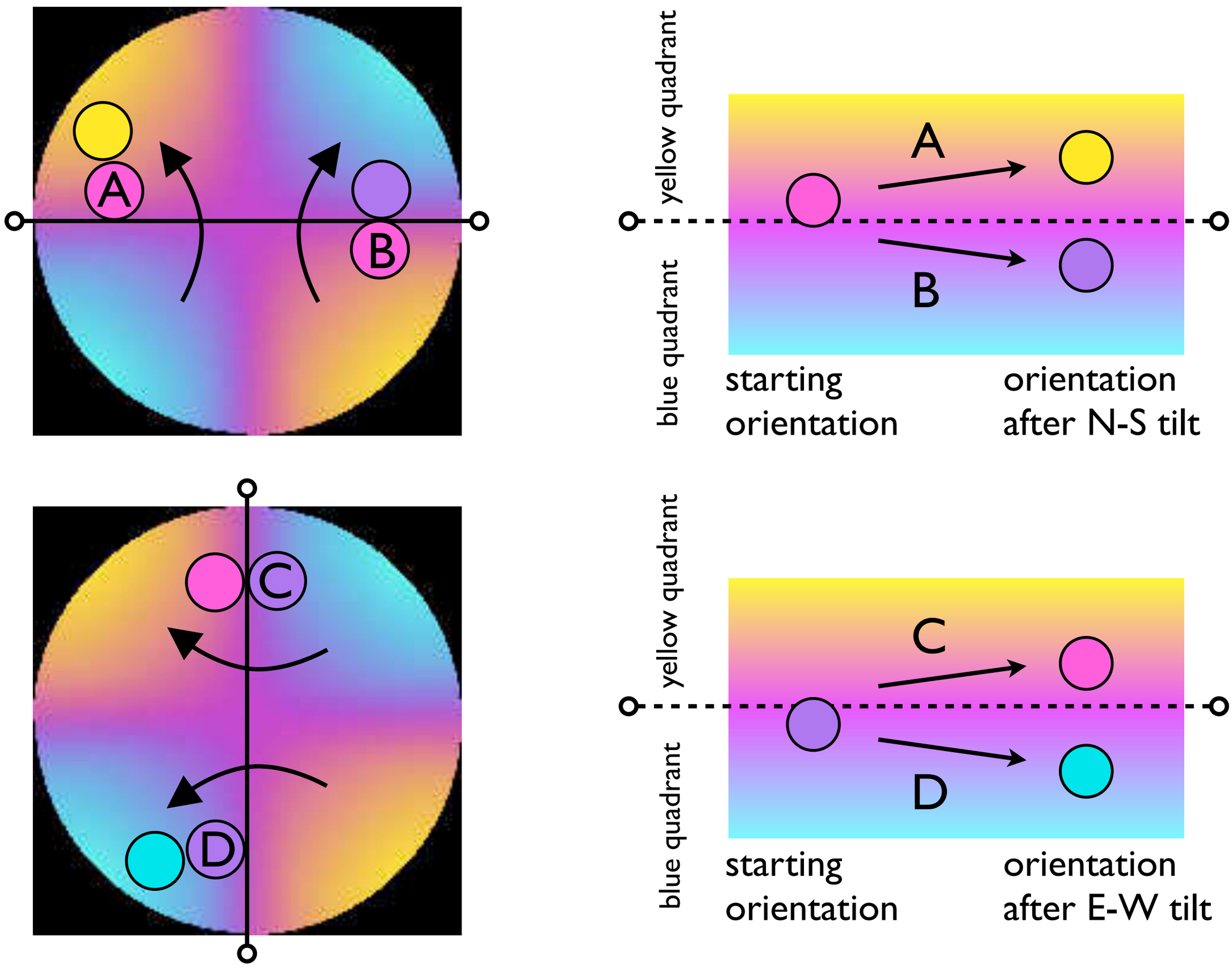

Figure 21.4
Deriving the full inclination.
Two tilts of the thin section define the starting orientation of given c-axes: a tilt about an E-W axis discriminates A (going towards yellow quadrant) from B (going towards blue quadrant); a tilt about an E-W axis discriminates C (going towards yellow quadrant) from D (going towards blue quadrant). The tilt operations are shown on the conoscopic image (left).

a

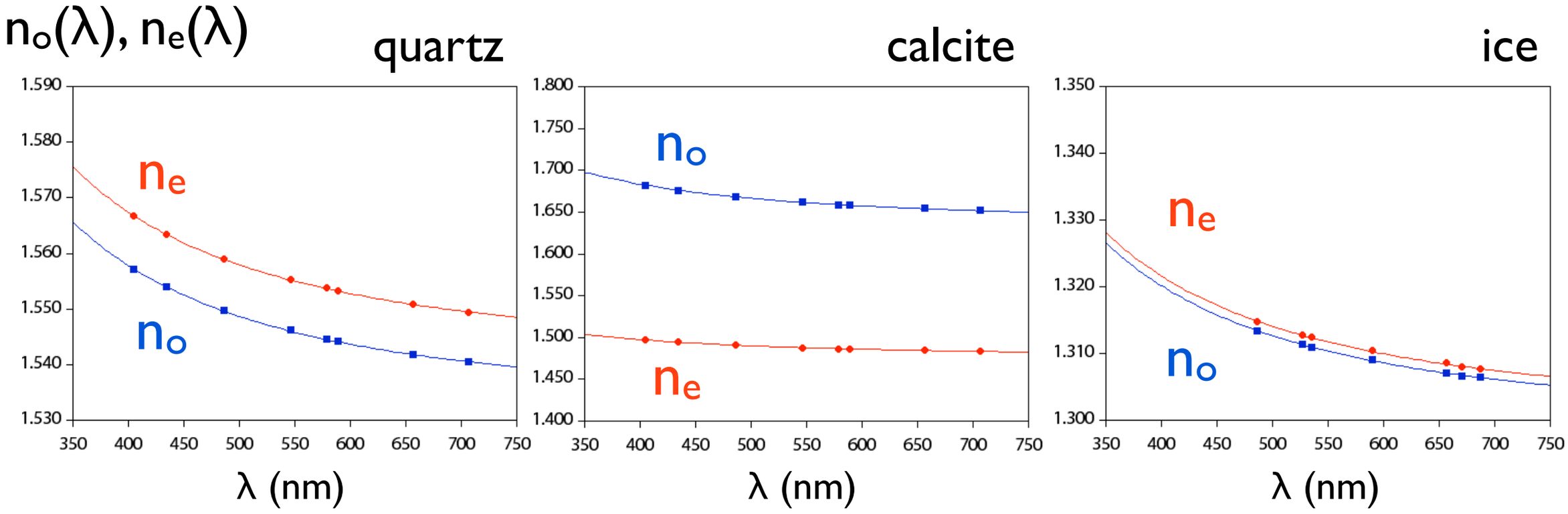

b

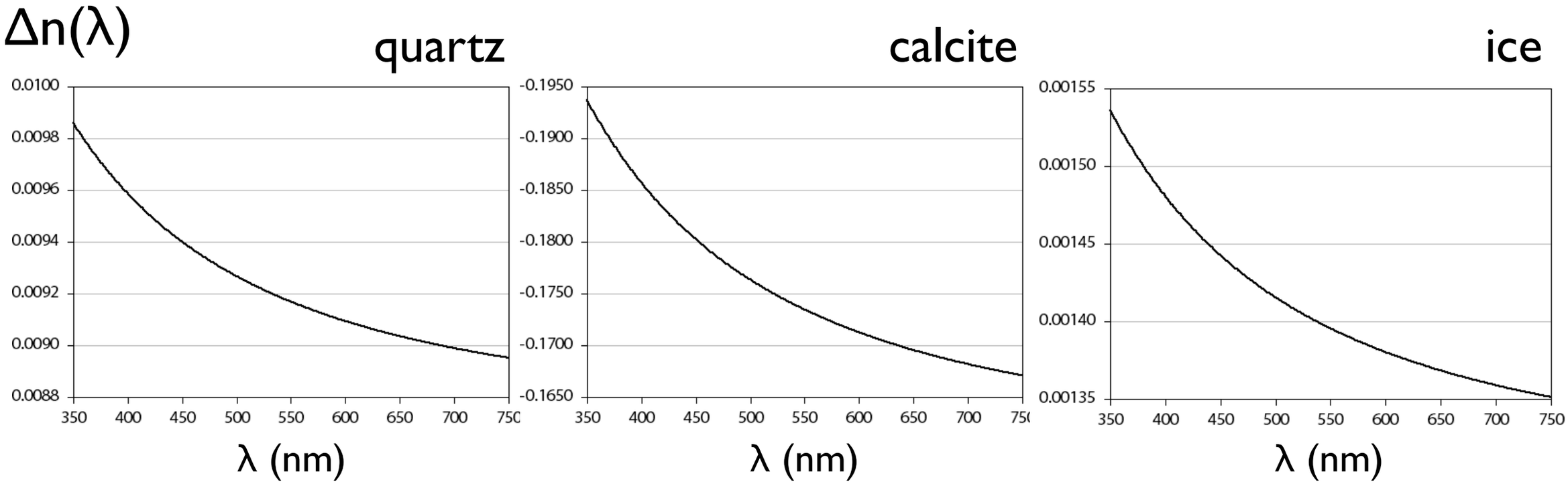

Figure 21.5
Refractive index and birefringence.
(a) Refractive index, n(λ), of quartz, calcite and ice as a function of wavelength; n_o, n_e = refractive index of ordinary and extraordinary ray, respectively;
(b) birefringence , $\Delta n(\lambda) = n_e - n_o$; if $n_e > n_o$, the mineral is positive, if $n_e < n_o$, it is negative.

quartz

nm	n_e	n_o	Δn
303.4120	1.58720	1.57695	0.01025
340.3650	1.57738	1.56747	0.00991
404.6560	1.56671	1.55716	0.00955
434.0470	1.56340	1.55396	0.00944
486.1330	1.55898	1.54968	0.00930
546.0720	1.55535	1.54617	0.00918
579.0660	1.55379	1.54467	0.00912
589.2900	1.55336	1.54425	0.00911
656.2780	1.55093	1.54190	0.00903
706.5200	1.54947	1.54049	0.00898
766.4940	1.54800	1.53907	0.00893

calcite

nm	n_e	n_o	Δn
303.4120	1.51366	1.71956	-0.20590
340.3650	1.50561	1.70080	-0.19519
404.6560	1.49694	1.68134	-0.18440
434.0470	1.49428	1.67552	-0.18124
486.1330	1.49076	1.66785	-0.17709
546.0720	1.48792	1.66186	-0.17394
579.0660	1.48674	1.65906	-0.17232
589.2900	1.48641	1.65836	-0.17195
656.2780	1.48461	1.65438	-0.16977
706.5200	1.48397	1.65207	-0.16810
800.7000	1.48212	1.64867	-0.16655

.

ice

nm	n_e	n_o	Δn
486.1340	1.31473	1.31335	0.00138
527.0390	1.31276	1.31140	0.00136
535.1000	1.31242	1.31098	0.00144
589.5940	1.31041	1.30911	0.00130
656.2810	1.30861	1.30715	0.00146
670.8000	1.30802	1.30669	0.00133
686.7190	1.30775	1.30645	0.00130
759.3700	1.30626	1.30496	0.00130

Table 21.1
Measured values of refractive indices of quartz, calcite and ice.
Refractive indices for extraordinary and ordinary ray, n_e and n_o, are given for selected wavelengths (nm); the birefringence, $\Delta n = n_e - n_o$.

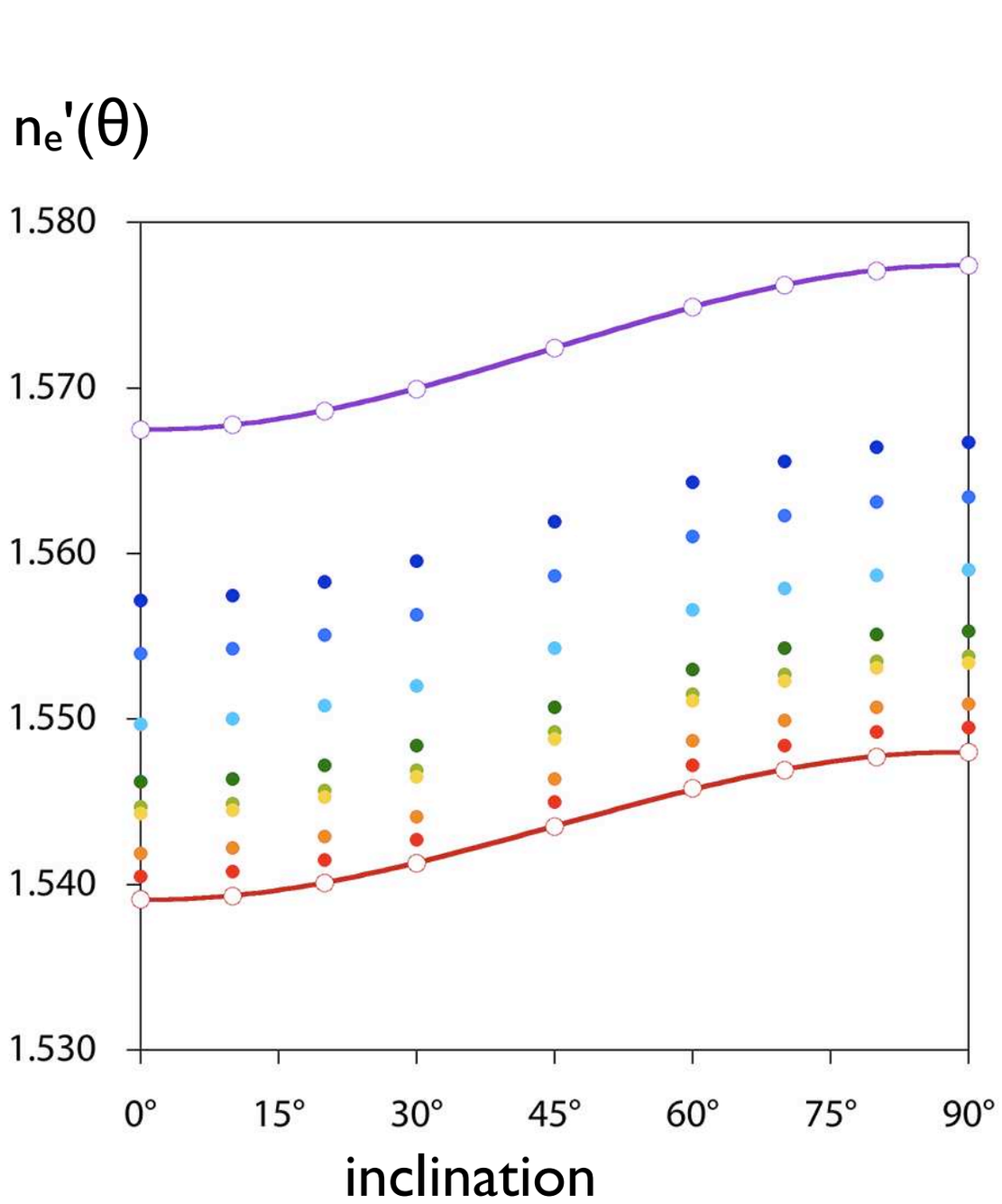

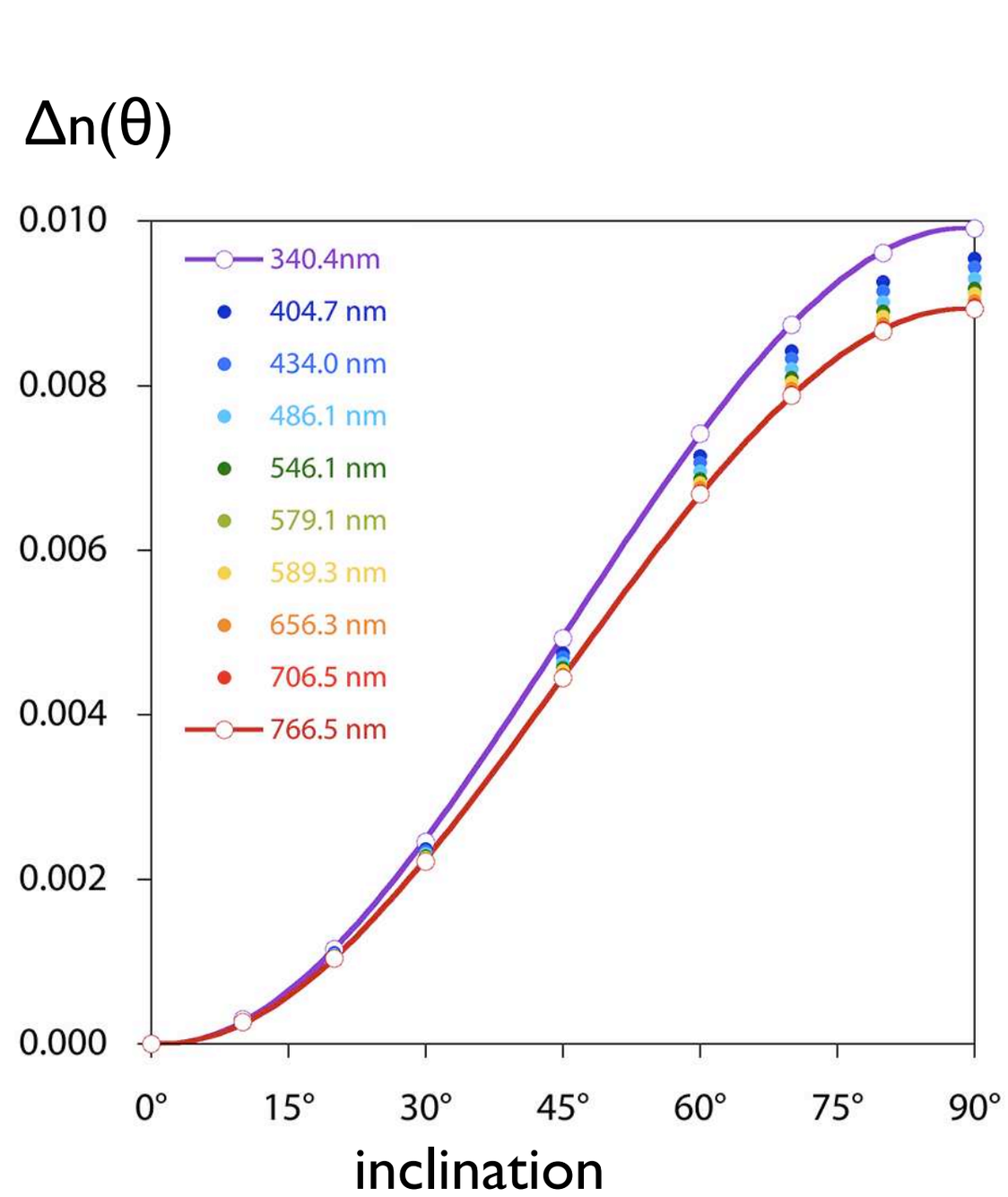

Figure 21.6
Inclination dependence of birefringence.
(a) Refractive index, $n_e'(\theta)$, of the extraordinary ray of quartz for ten different wavelengths (from λ = 340.4 nm to 766.5 nm); note that at $\theta = 0°$, the values $n_e'(\lambda) = n_o(\lambda)$, and at $\theta = 90°$, $n_e'(\lambda) = n_e(\lambda)$;
(b) birefringence, $\Delta n(\theta)$, for the same ten wavelengths as (a); note that at $\theta = 0°$, $\Delta n(\lambda) = 0.00$, and at $\theta = 90°$, $\Delta n(\lambda)$ = maximum value = $n_e(\lambda) - n_o(\lambda)$.

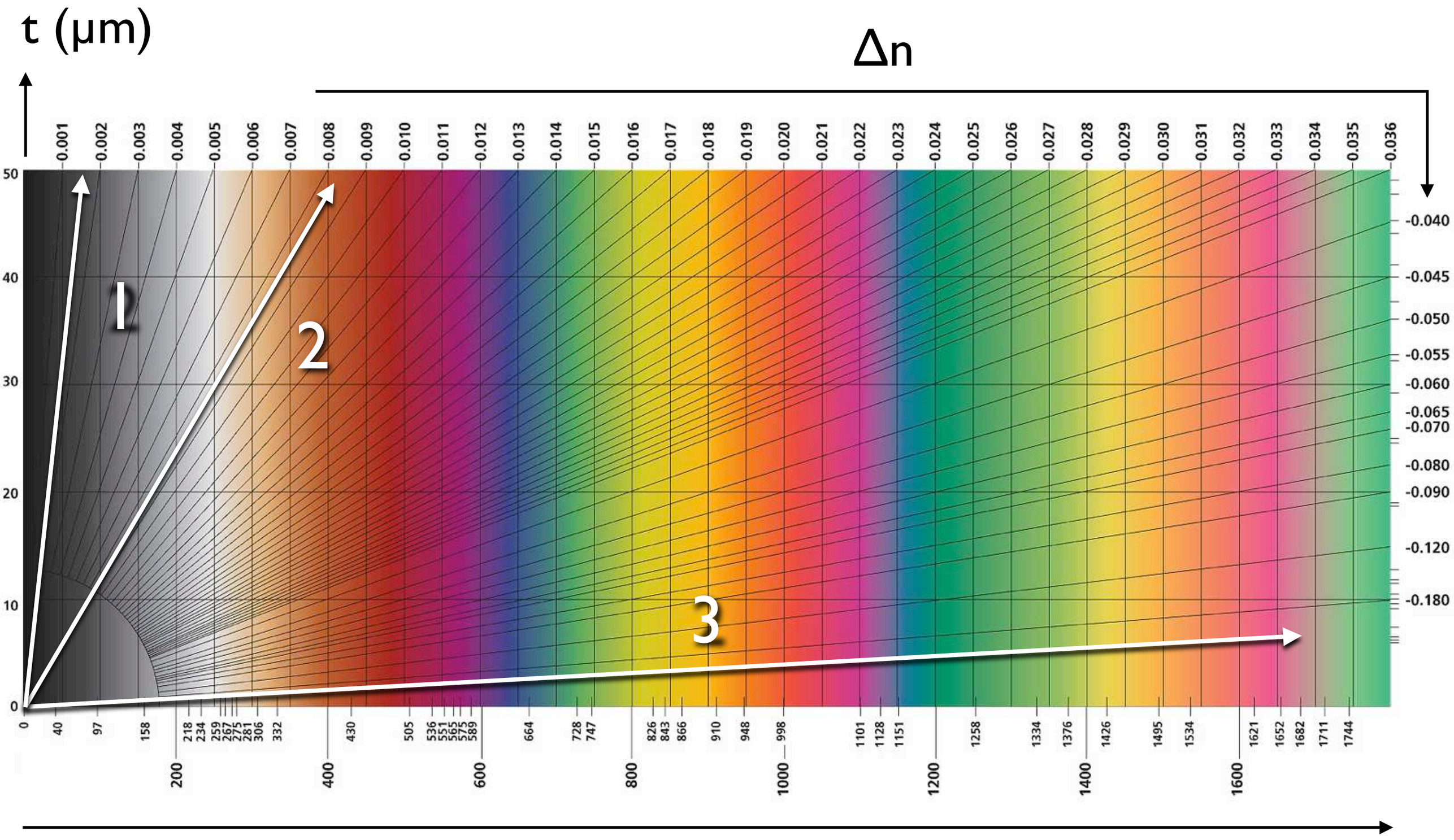

Figure 21.7
Michel-Lévy chart.
Color impression shown as a function of thickness of section and relative optical path length, R. Rays indicate interference colors for minerals with given birefringence, Δn: 1 = ice, 2 = quartz, 3 = calcite and dolomite. From left to right, red dots indicate 1st, 2nd and 3rd order of interference color; each order = 550 nm.

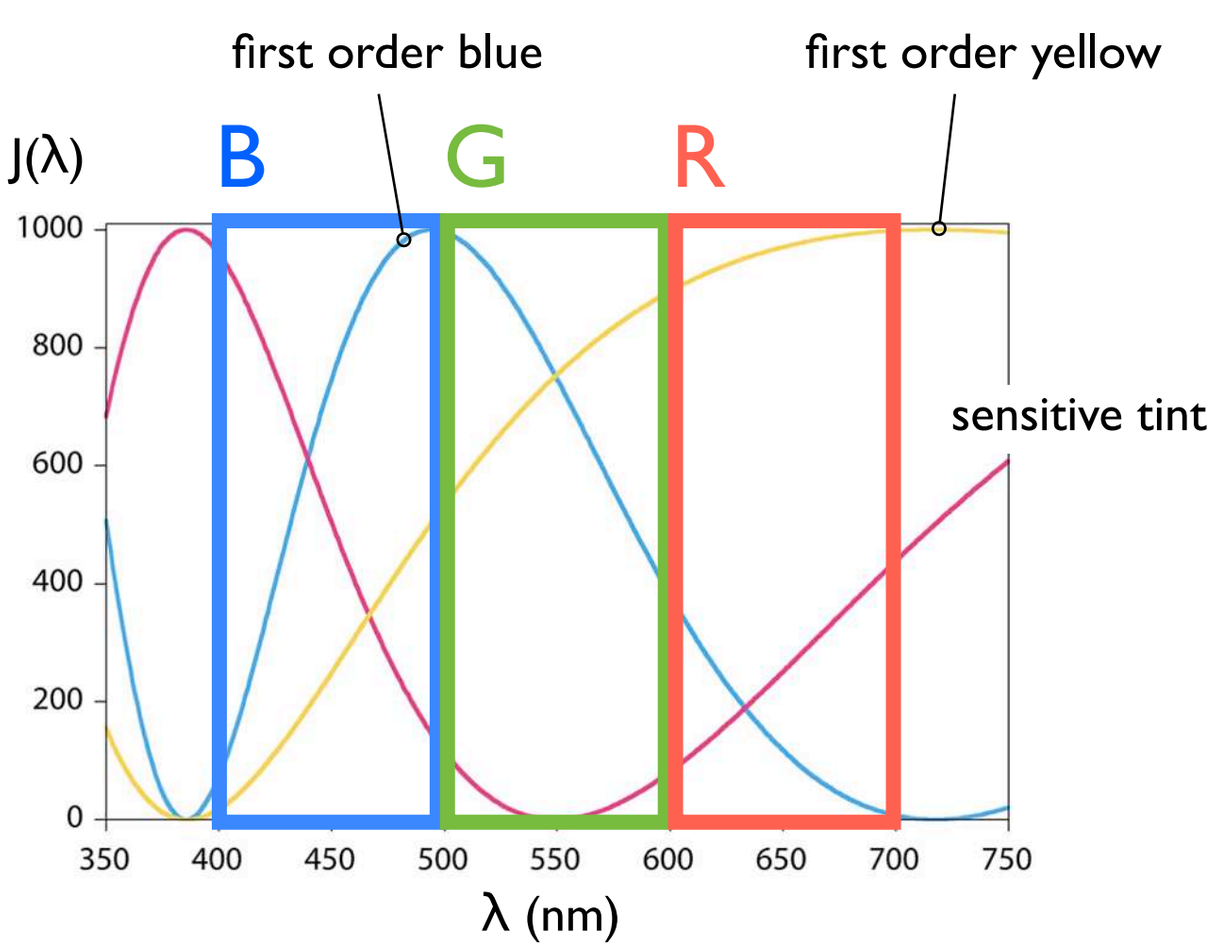

Figure 21.8
Converting spectra to color.
Simplified concept of additive color mixing from Red Green and Blue part of spectrum: 1= first-order blue, mainly composed of B and G, appears cyan; 2= first-order yellow, composed of G and R, appears yellow; 3 = sensitive tint, composed of B and R, appears magenta.

a

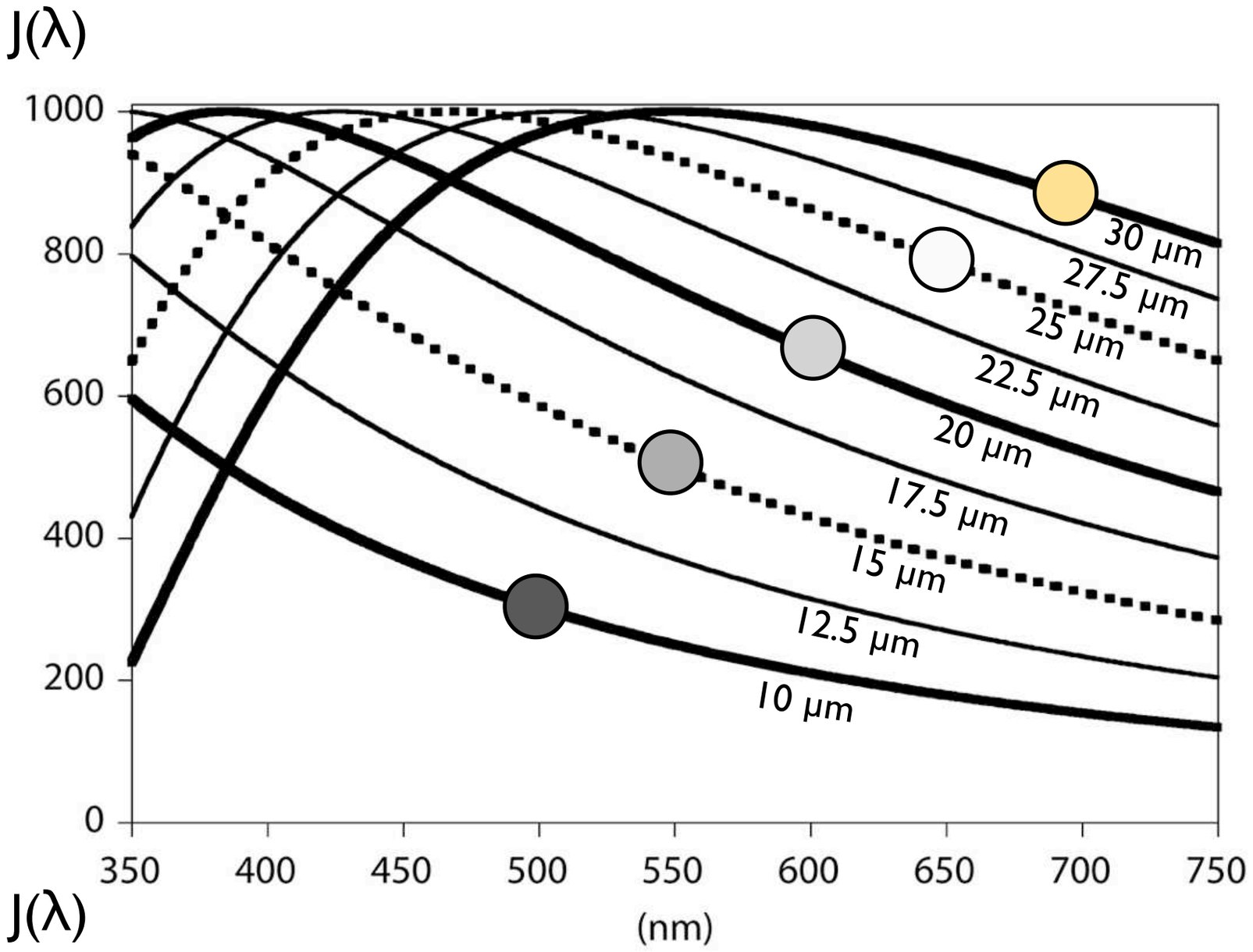
J(λ)
1000
800
600
400
200
0
350
400
450
500
550
600
650
700
750
(nm)
30 μm
27.5 μm
25 μm
22.5 μm
20 μm
17.5 μm
15 μm
12.5 μm
10 μm

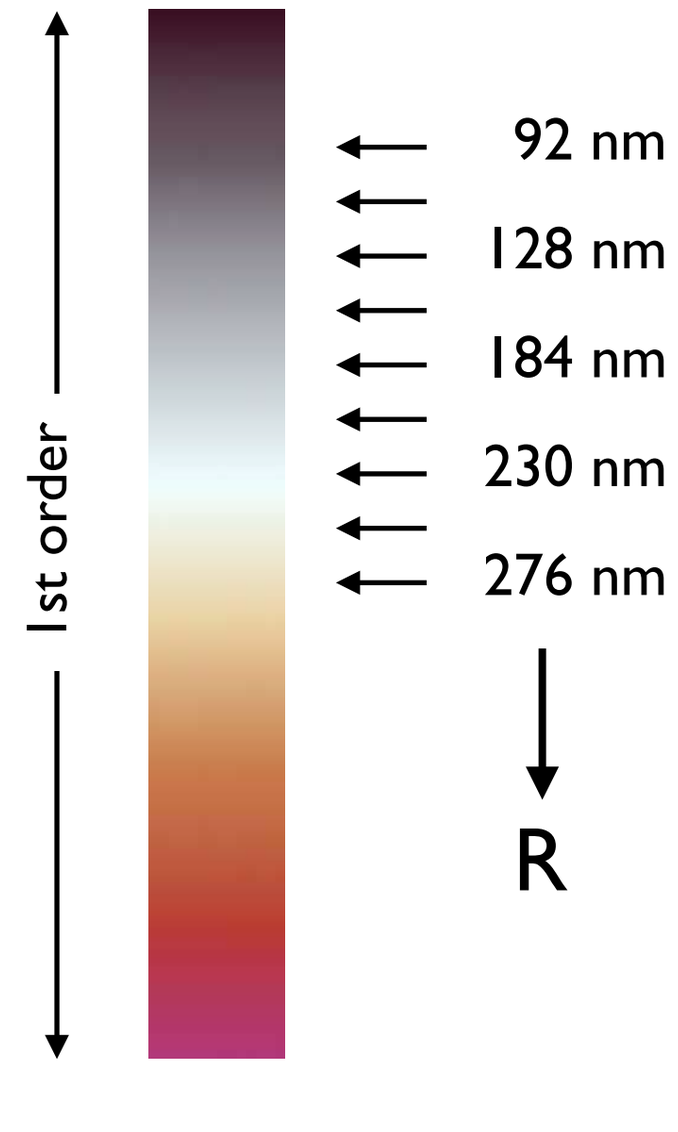
1st order
92 nm
128 nm
184 nm
230 nm
276 nm
R

b

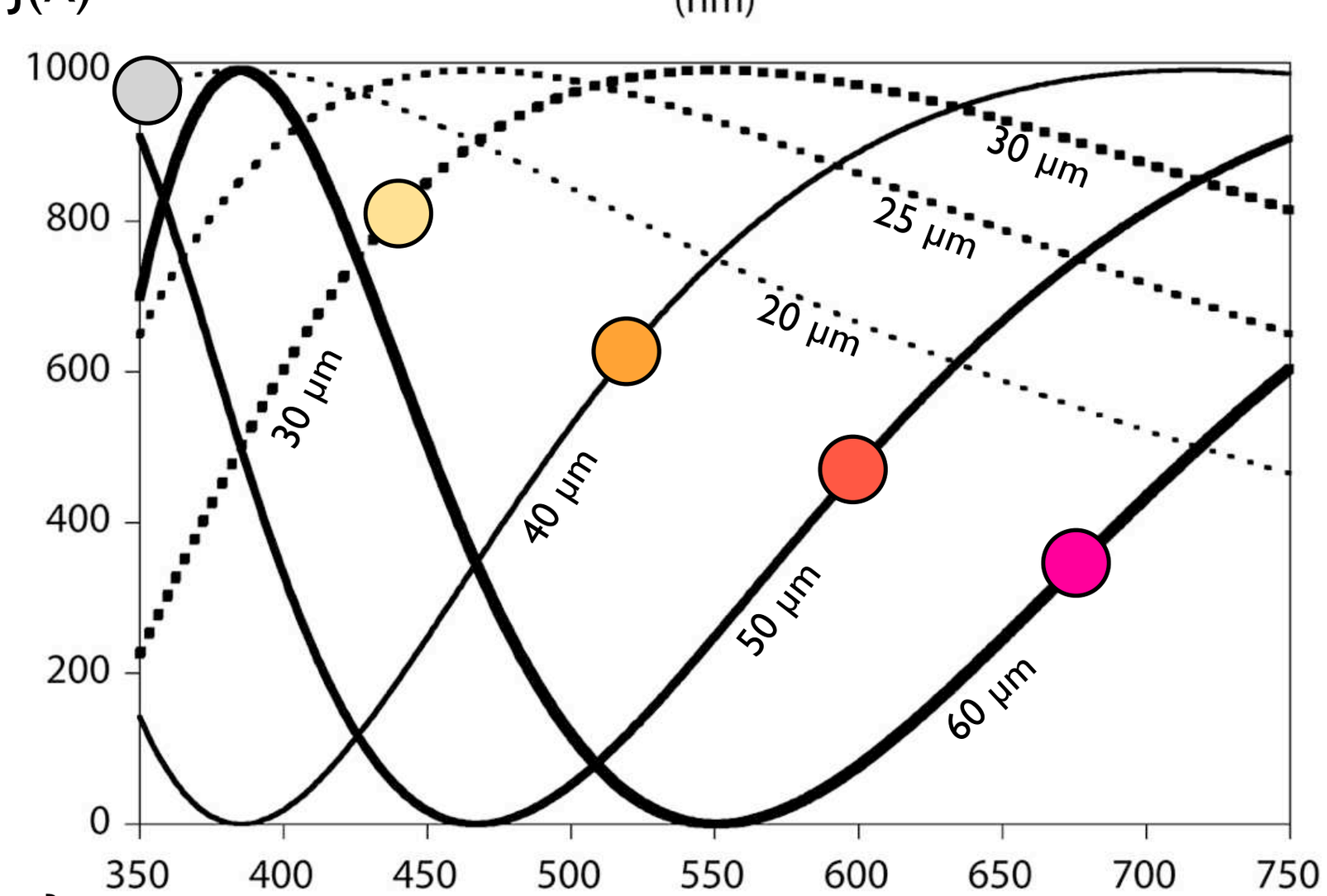
J(λ)
1000
800
600
400
200
0
350
400
450
500
550
600
650
700
750
(nm)
30 μm
25 μm
20 μm
40 μm
50 μm
60 μm

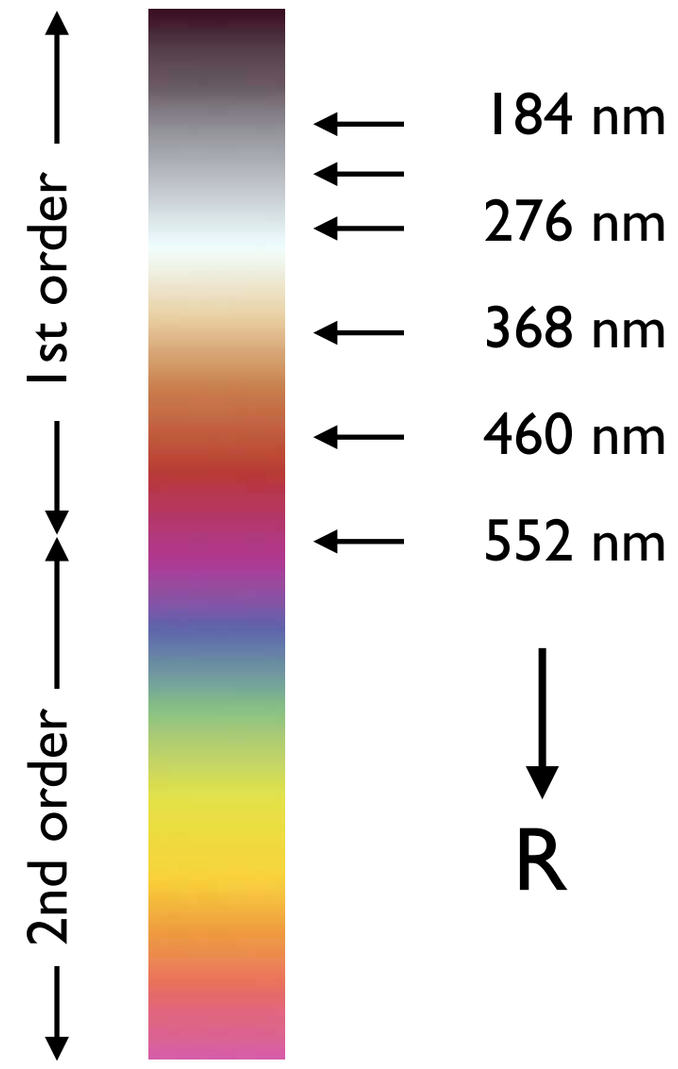
1st order
2nd order
184 nm
276 nm
368 nm
460 nm
552 nm
R

c

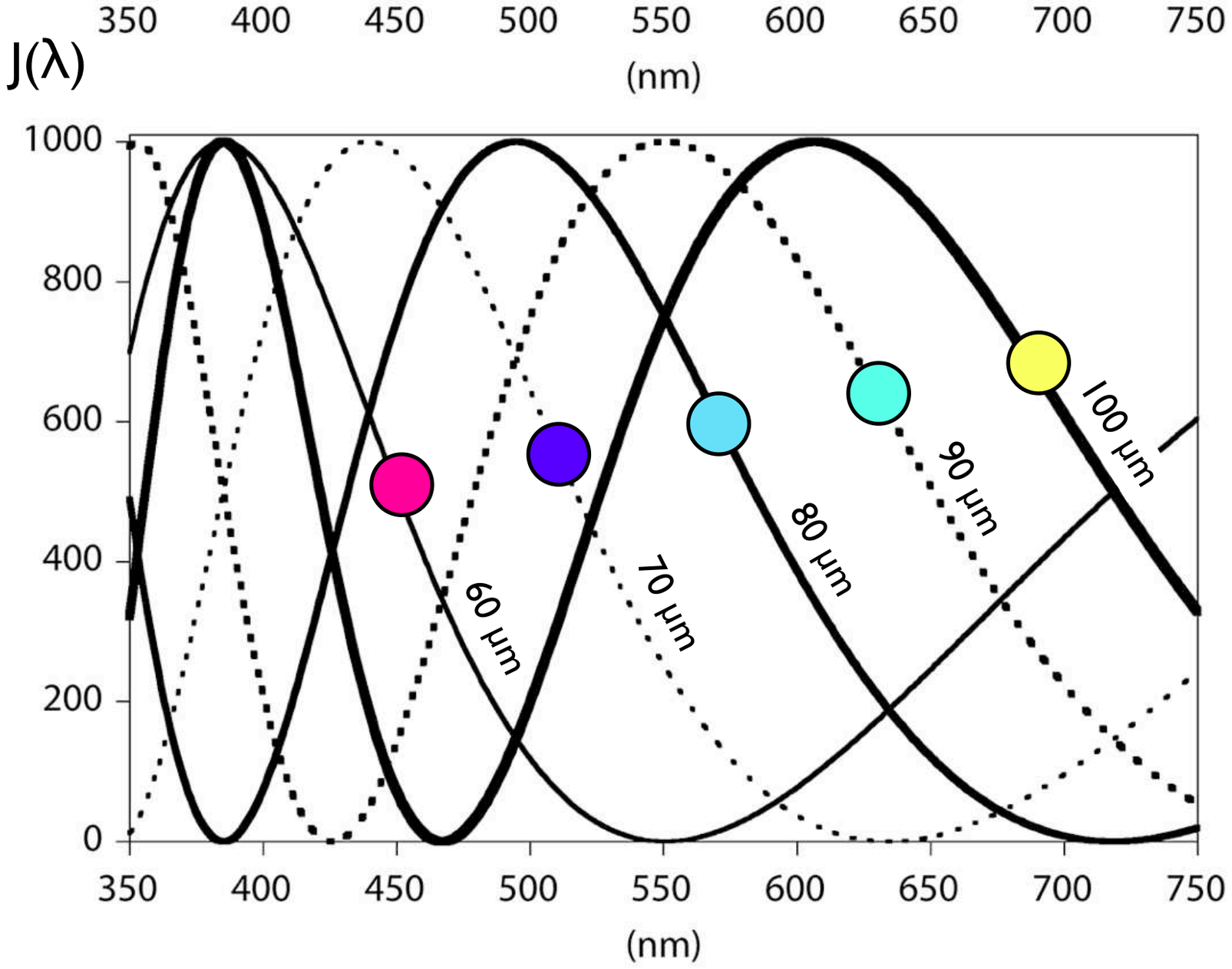
J(λ)
1000
800
600
400
200
0
350
400
450
500
550
600
650
700
750
(nm)
60 μm
70 μm
80 μm
90 μm
100 μm

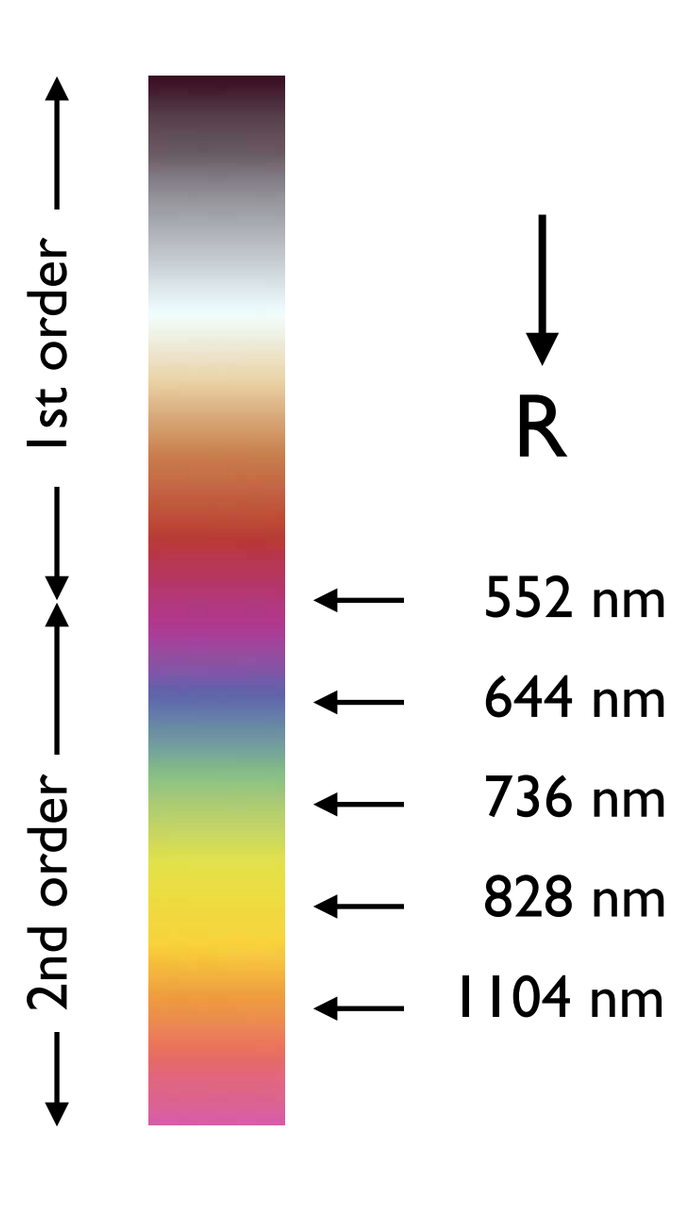
1st order
2nd order
552 nm
644 nm
736 nm
828 nm
1104 nm
R

Figure 21.9
Spectra of interference colors of quartz.
Relative intensity, J, as function of wavelength, λ, for thin sections of quartz; section thickness is indicated in µm; the approximate color impressions of the spectra are indicated by small circles on the curves; to the right, a color chart (Michel-Lévy chart) for increasing relative optical path length, R, is shown.
(a) Thin sections of 10 - 30 µm thickness;
(b) 20 - 60 µm;
(c) 60 - 100 µm.

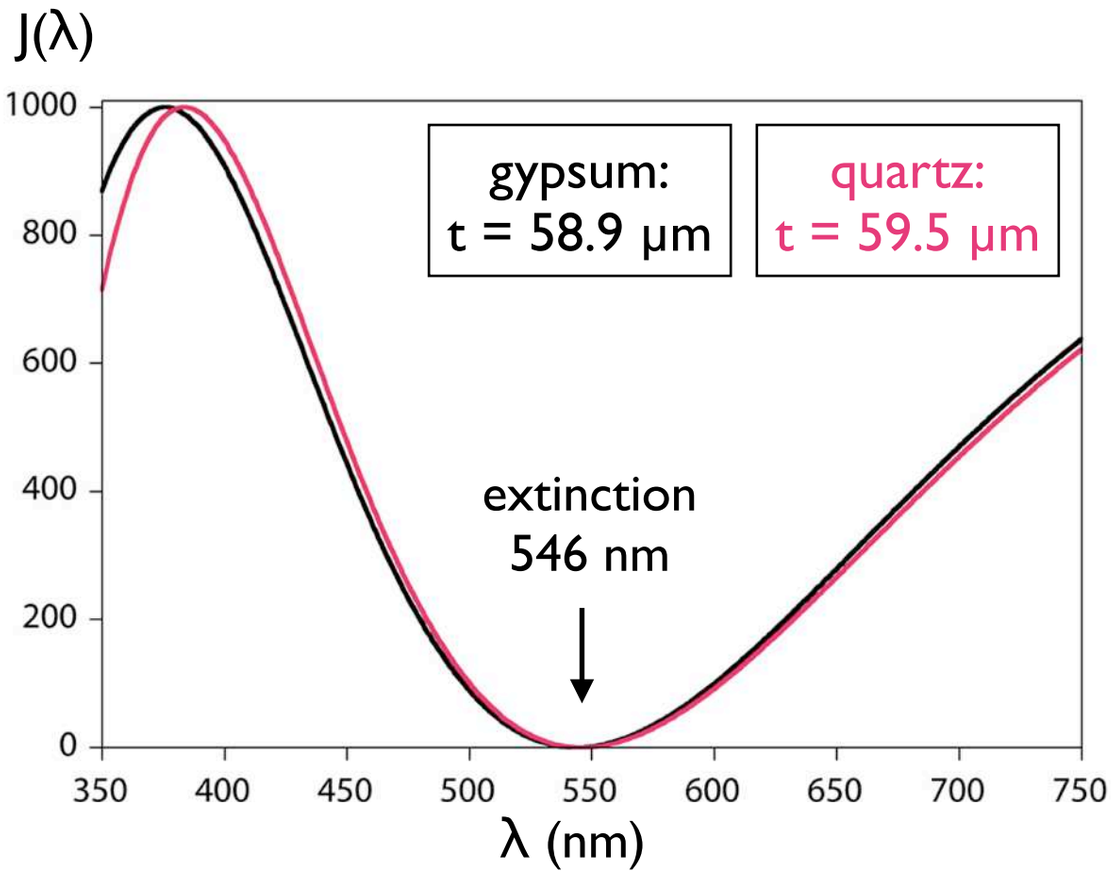

Figure 21.10
Spectrum of sensitive tint.
Spectra for wave plates made from quartz and gypsum are shown.

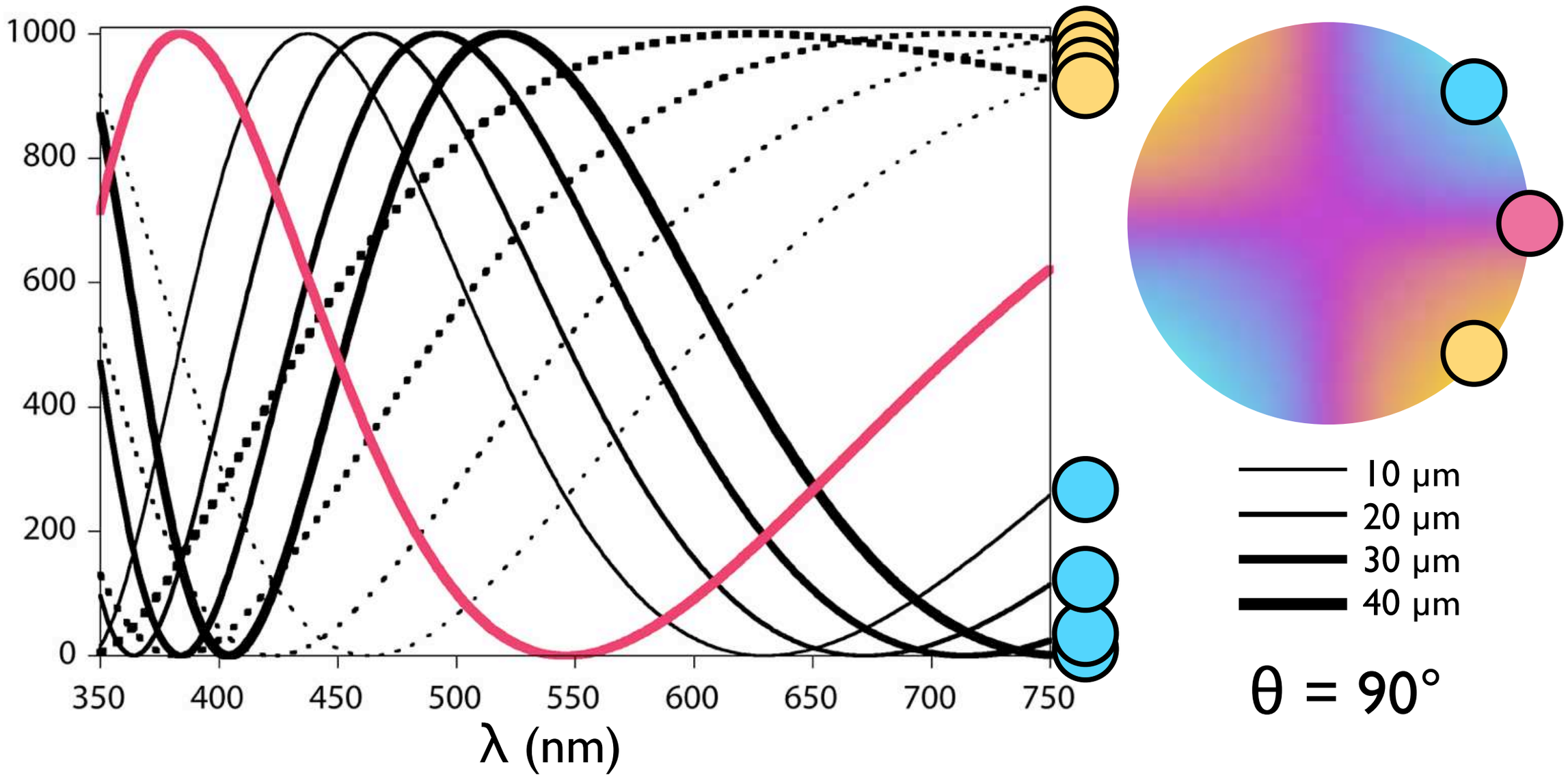

Figure 21.11
Interference colors of quartz for different section thickness.
Spectra for quartz under cross polarization with the wave plate inserted; thickness of section varies from 10 to 30 µm. The optic axis of quartz is in the plane of the section; the azimuth, measured form North, is φ = 45° (blue), 90° (magenta, sensitive tint) and 135° (yellow); the inclination, θ = 90°, is measured from the section normal. The orientation of the optic axes is plotted on the conoscopic image (stereographic projection of interference color).

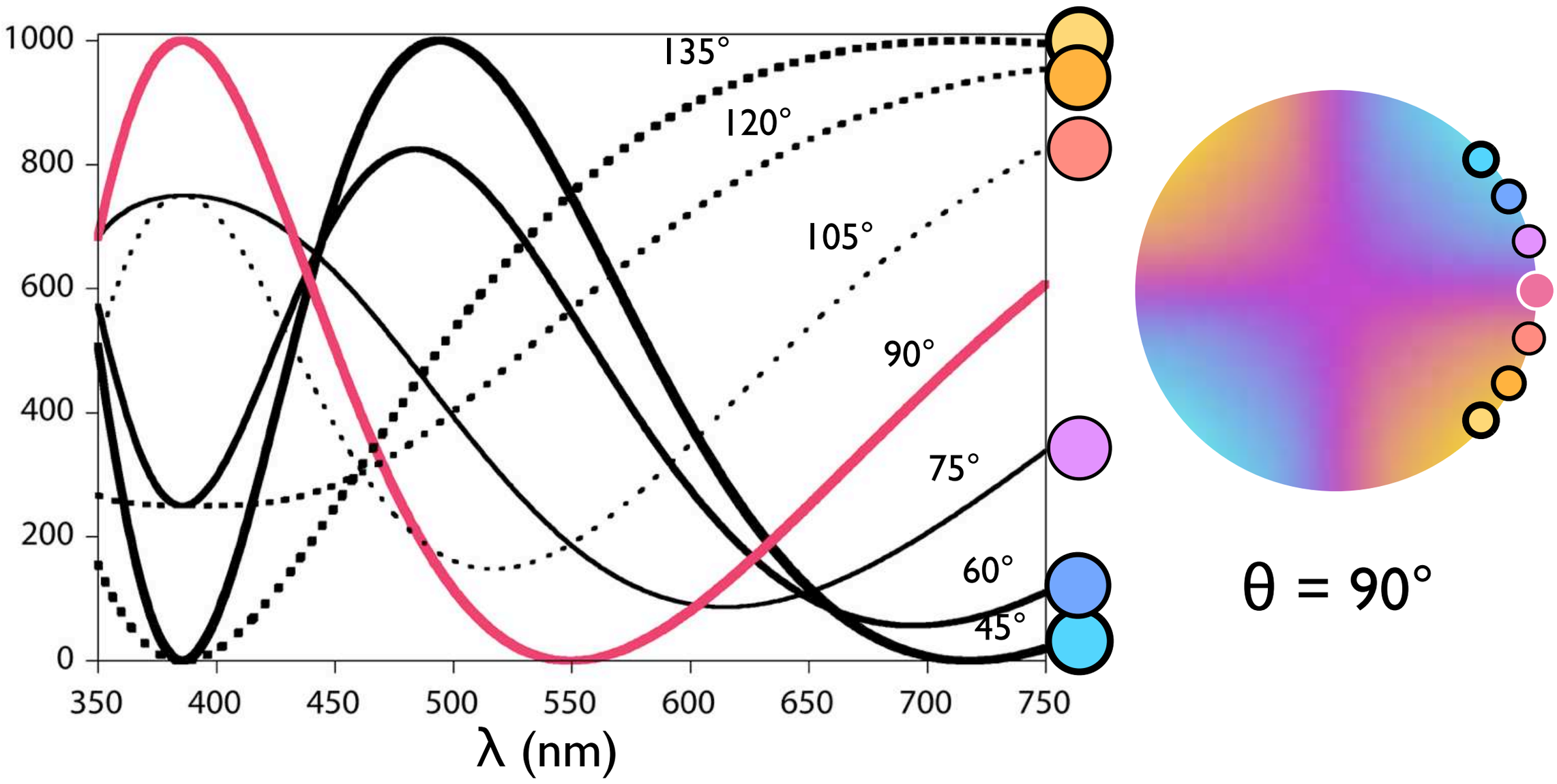

Figure 21.12
Interference colors of quartz for varying azimuth of optic axis.
Spectra for quartz under cross polarization with the wave plate inserted; thickness of section is 20 μm. The azimuth, φ, is measured from North, varying from 45° (blue) to 135° (yellow); the inclination, θ, is 90°. The orientations of the optic axes are also shown on the conoscopic image on the right.

a

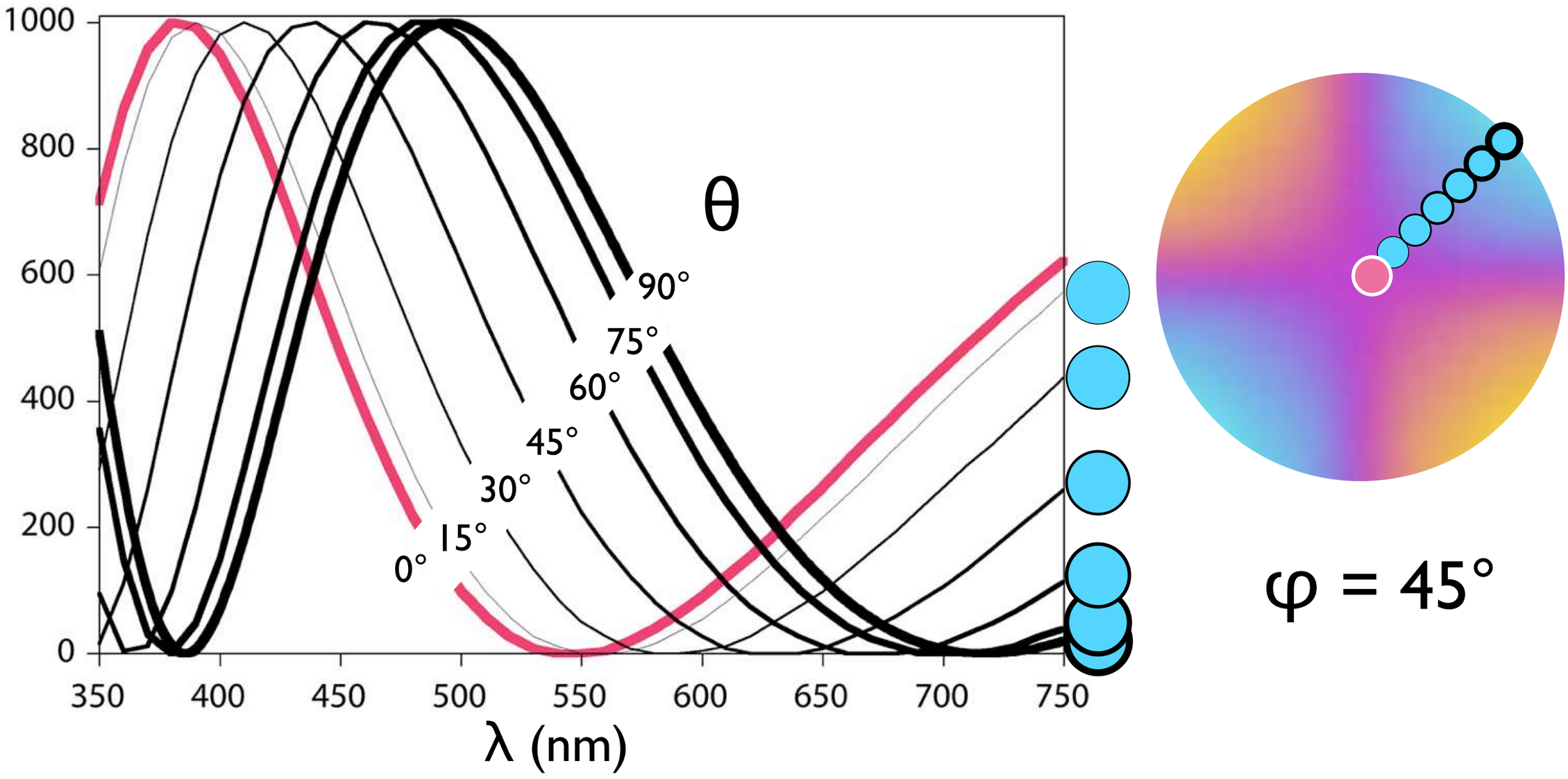

b

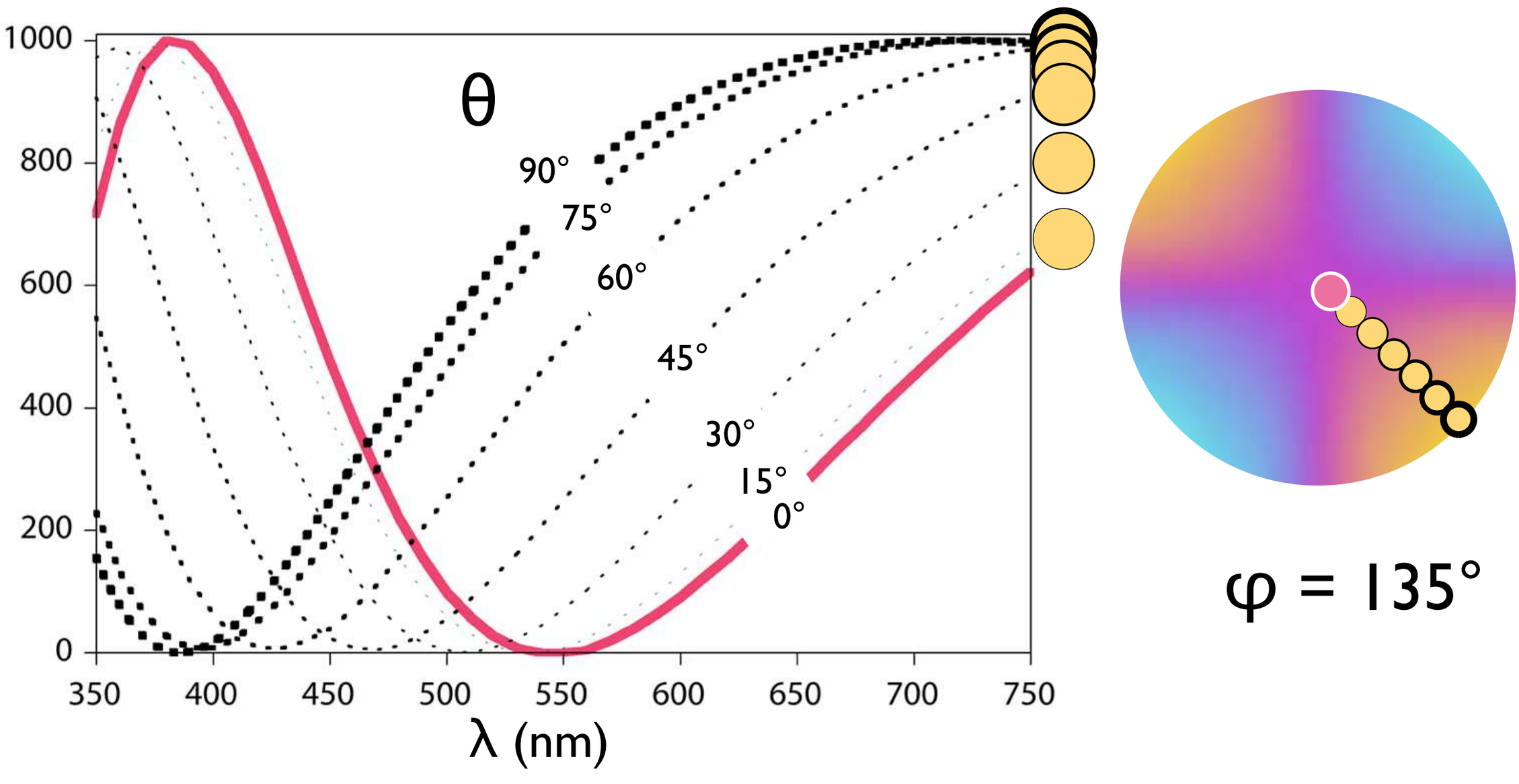

Figure 21.13
Interference colors of quartz for varying inclination of optic axis.
Spectra for quartz under cross polarization with the wave plate inserted; thickness of section is 20 μm. The azimuth, φ, is measured from North, the inclination, θ, is 90°, from the section normal. The orientations of the optic axes are also shown on the conoscopic image on the right.
(a) Inclination, θ, varies from 0° to 90°, azimuth, φ, is 45° (blue);
(b) inclination, θ, varies from 0° to 90°, azimuth, φ, is 135° (yellow).

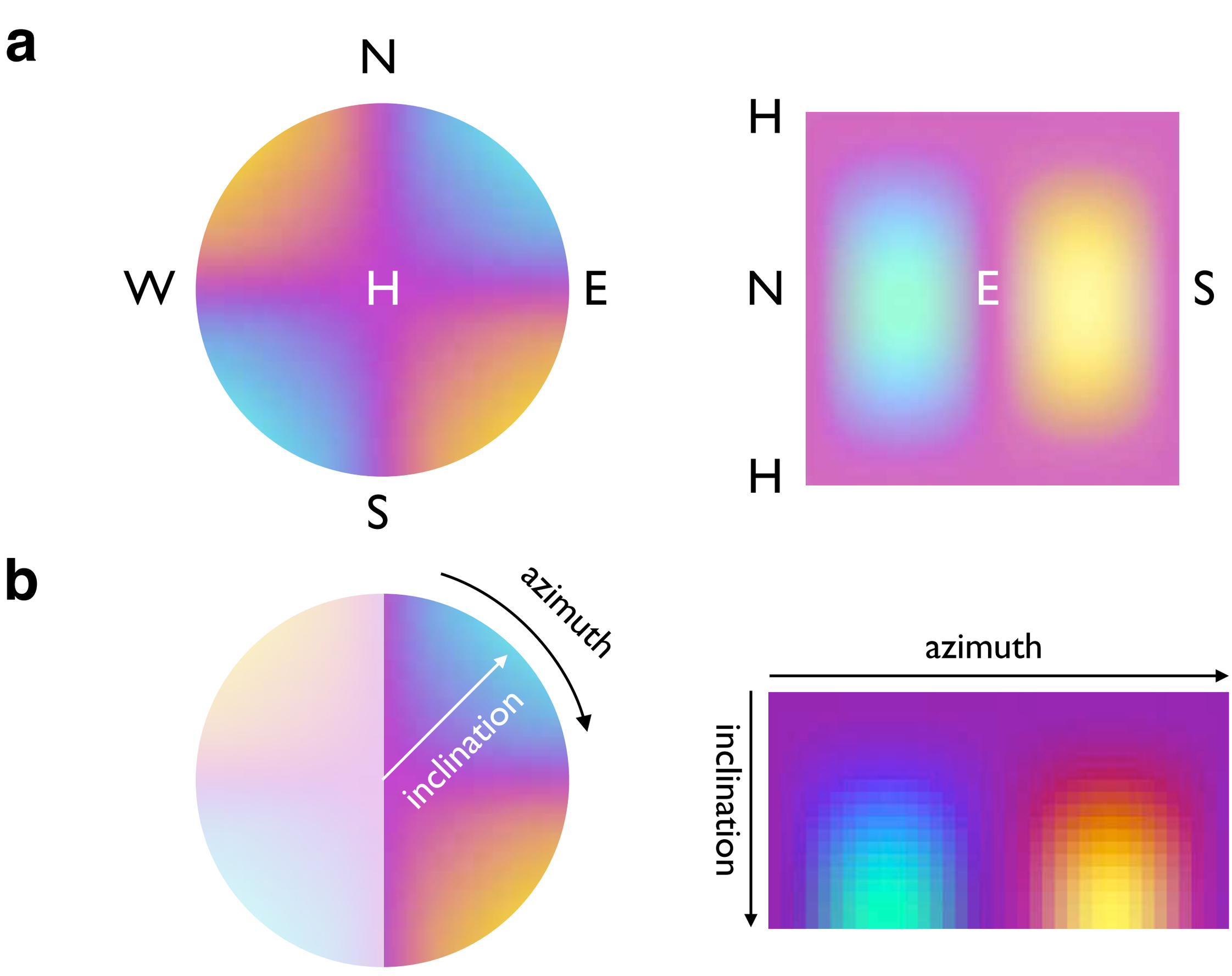

Figure 21.14
Interference color as a function of azimuth and inclination.
(a) Conoscopic image of quartz (= stereographic projection of interference colors) with orthogonal projection on the right.
(a) half of orientation halfspace: interference colors for azimuth ($0° \leq \varphi \leq 180°$) and inclination ($0° \leq \theta \leq 90°$); corresponding azimuth-inclination matrix (5° binning).

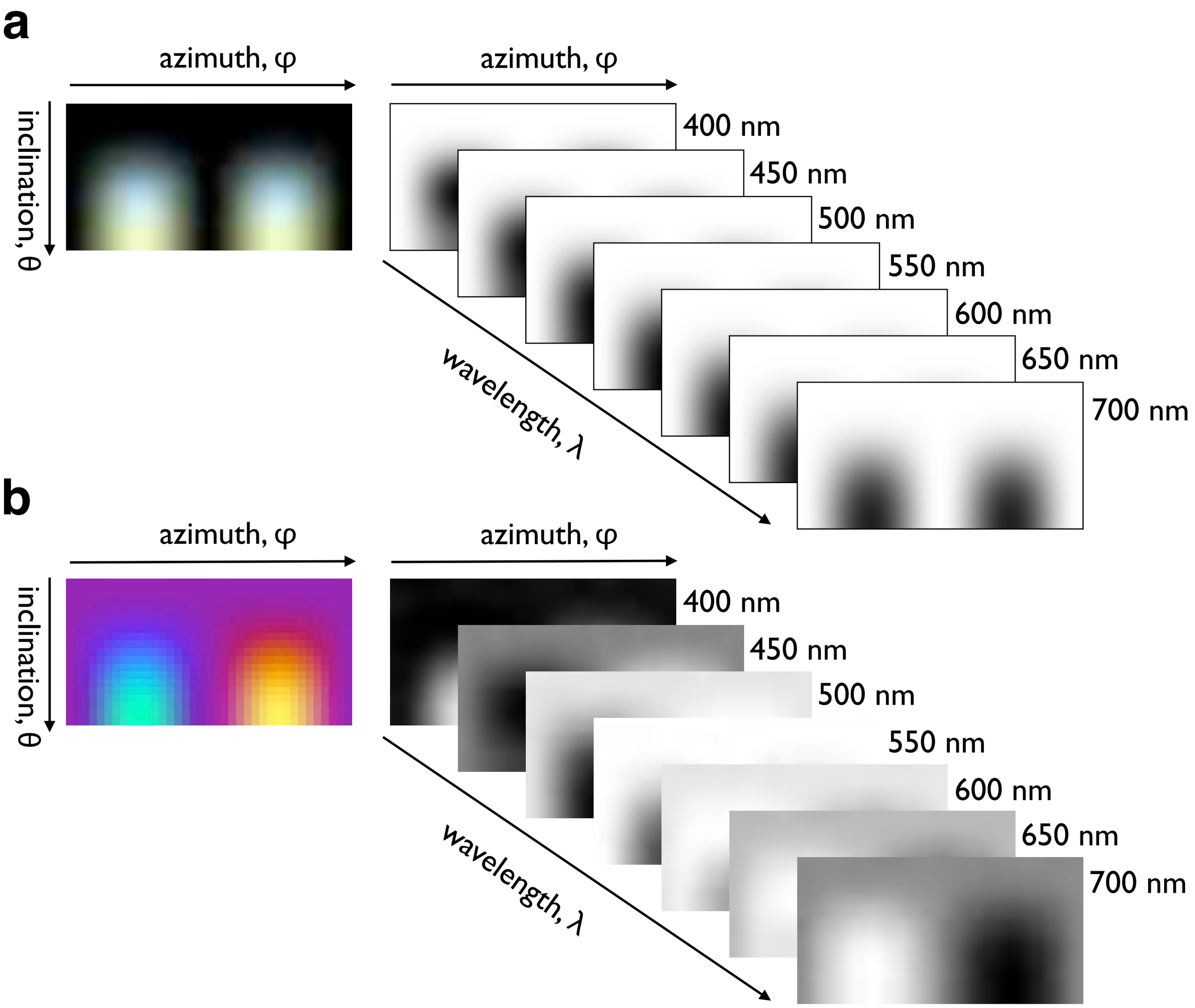

Figure 21.15
'Polstacks'.
Interference colors are calculated as intensity functions, J (λ, φ, θ), for wavelengths (350nm $\leq \lambda \leq$ 750nm), azimuths (0° $\leq \varphi \leq$ 180°) and inclinations (0° $\leq \theta \leq$ 90°), using a binning of 10nm for the wavelength and 5° for azimuth and inclination. The resulting 3-D matrix (41 · 37 · 19) is represented as an image stack ('polstack') with 41 slices, each representing the relative monochrome intensities, J(φ, θ), as a 37 · 19 gray value matrix. Note that gray value encoding renders high intensities as black.
(a) Polstack for quartz of 20 µm thickness under cross polarization;
(b) polstack for quartz of 20 µm thickness under cross polarization with wave plate added.

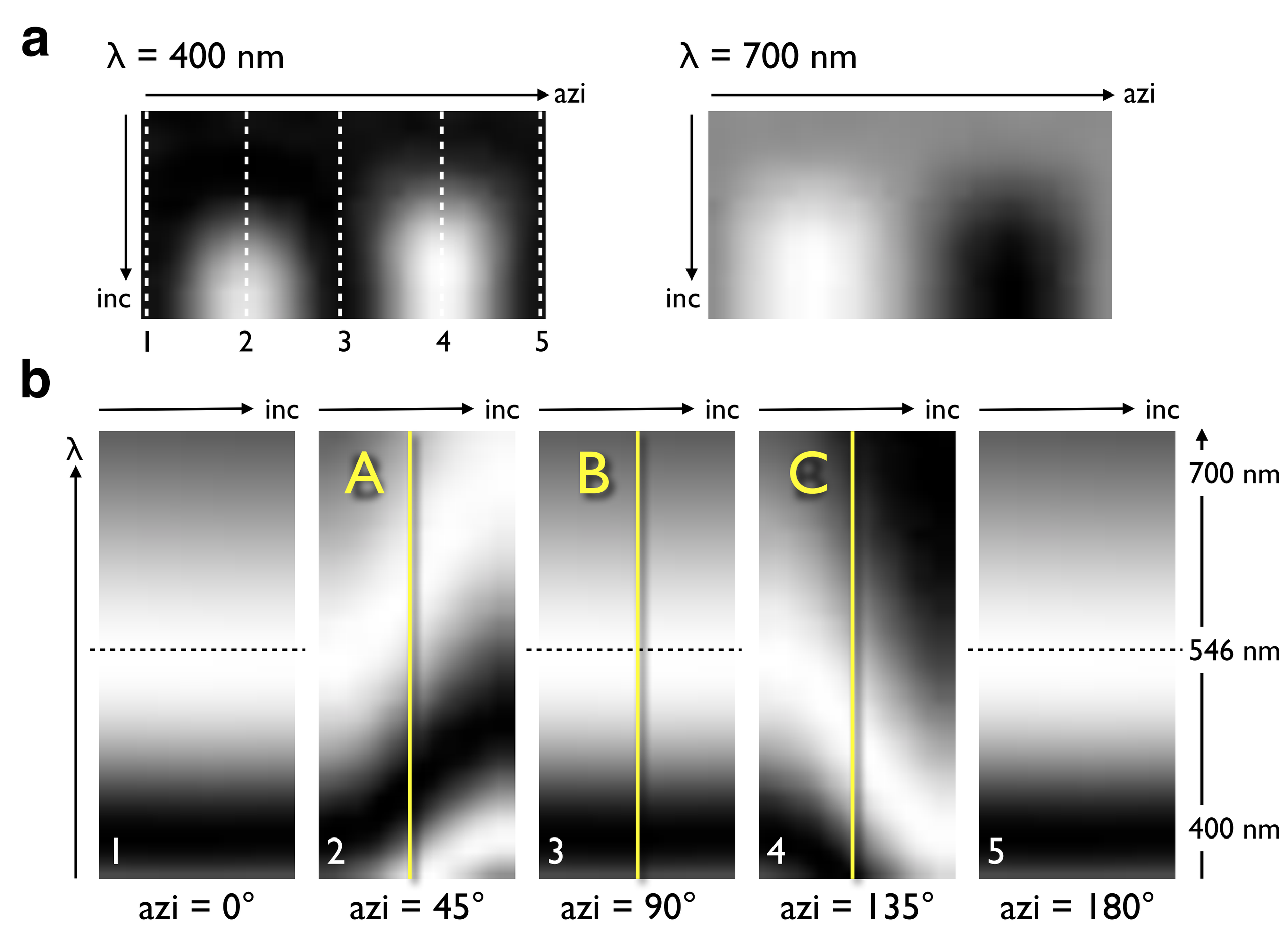

Figure 21.16
Inclination - wavelength sections.
Polstack calculated for quartz, 20 µm thickness, crossed polarizers and wave plate inserted; five (θ-λ) sections at constant azimuth (φ) are presented.
(a) (φ-θ) slices of the polstack: slice 6 (λ = 400 nm) and slice 36 (λ = 700 nm); traces for vertical (θ-λ) sections are shown;
(b) (θ-λ) sections for constant azimuths (φ = 0°, 45°, 90°, 135° and 180°).
Note that gray value encoding renders high intensities as black; the wavelength (546 nm) of zero intensity for the sensitive tint is indicated by black stippled line; A, B, C = traces for profiles shown in Figure 21.18.a.

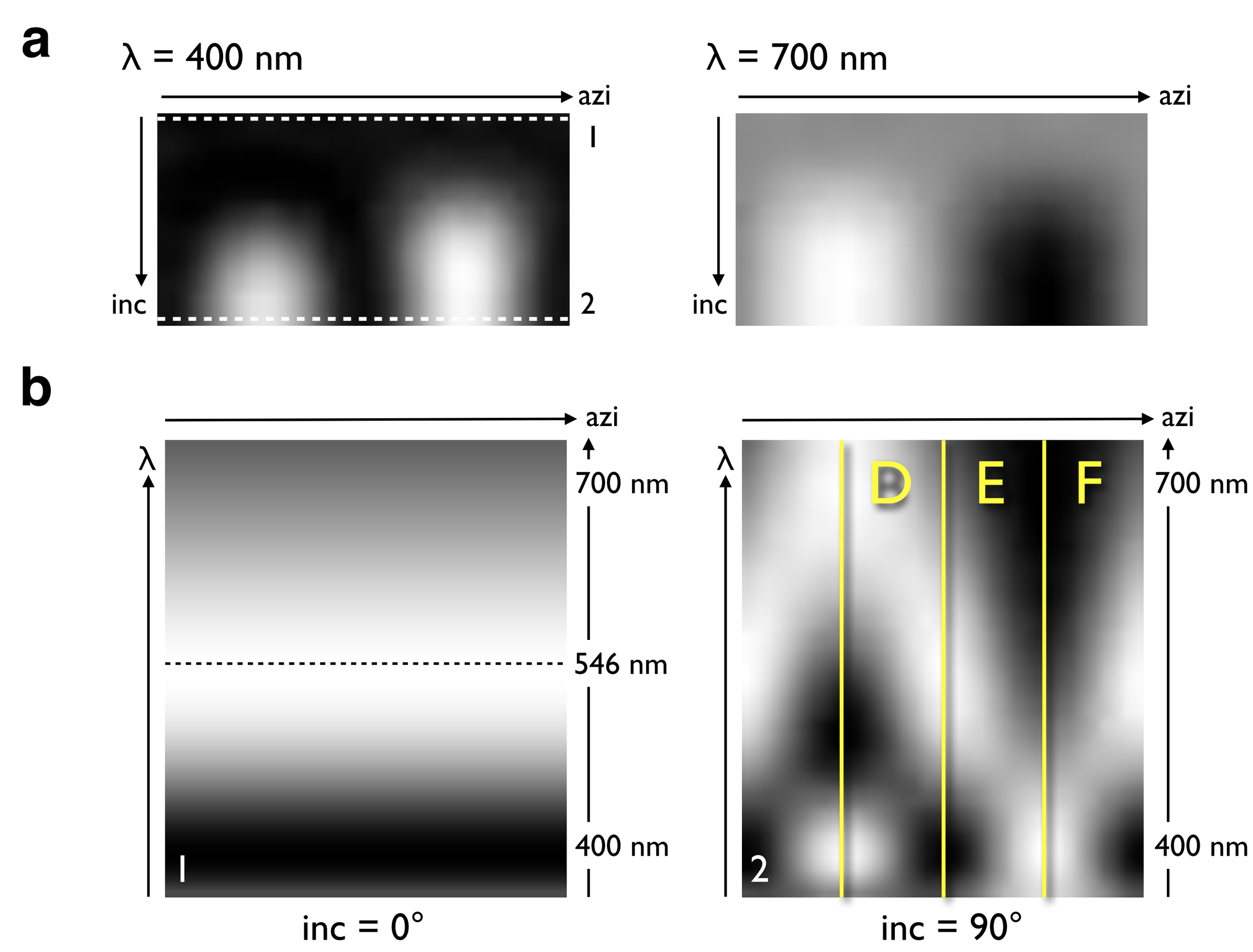

Figure 21.17
Azimuth - wavelength sections.
Polstack calculated for quartz, 20 µm thickness, crossed polarizers and wave plate inserted; two (φ -λ) sections at constant inclination (θ) are presented.
(a) (φ-θ) slices of the polstack: slice 6 (λ = 400 m) and slice 36 (λ = 700 nm); traces for vertical (φ-λ) sections are shown;
(b) (φ-λ) sections for constant inclinations (θ = 0° and 90°).
Note that gray value encoding renders high intensities as black; the wavelength (546 nm) of zero intensity for the sensitive tint is indicated; D, E, F = traces for profiles shown in Figure 21.18.b.

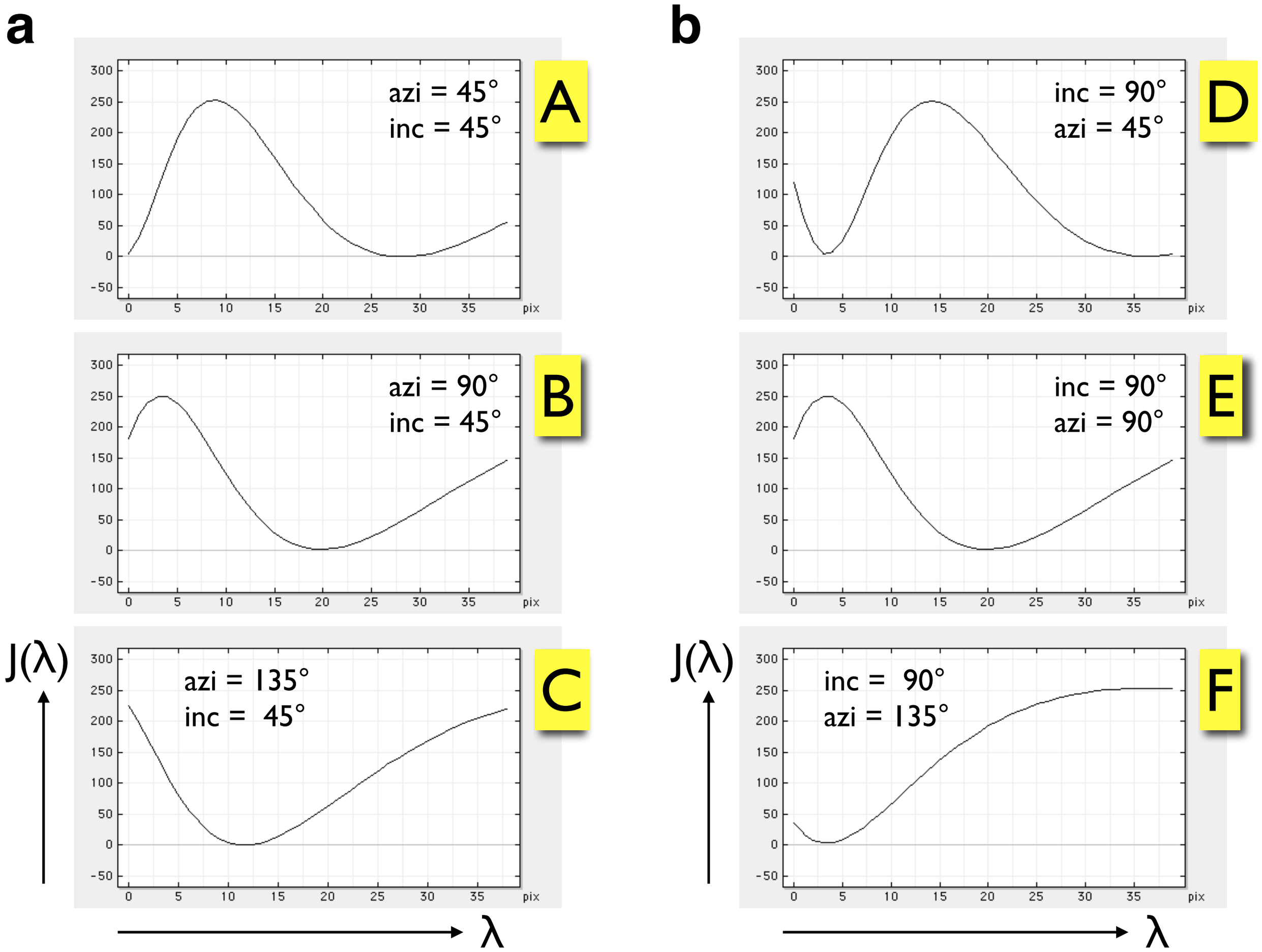

Figure 21.18
Spectra from polstack sections.
(a) Profiles along traces A, B, C on inclination-wave-length sections at φ = 45°, 90°, and 135° (Figure 21.16.b);
(b) profiles along traces D, E, F on azimuth-wave-length section at θ = 90° (Figure 21.17.b).

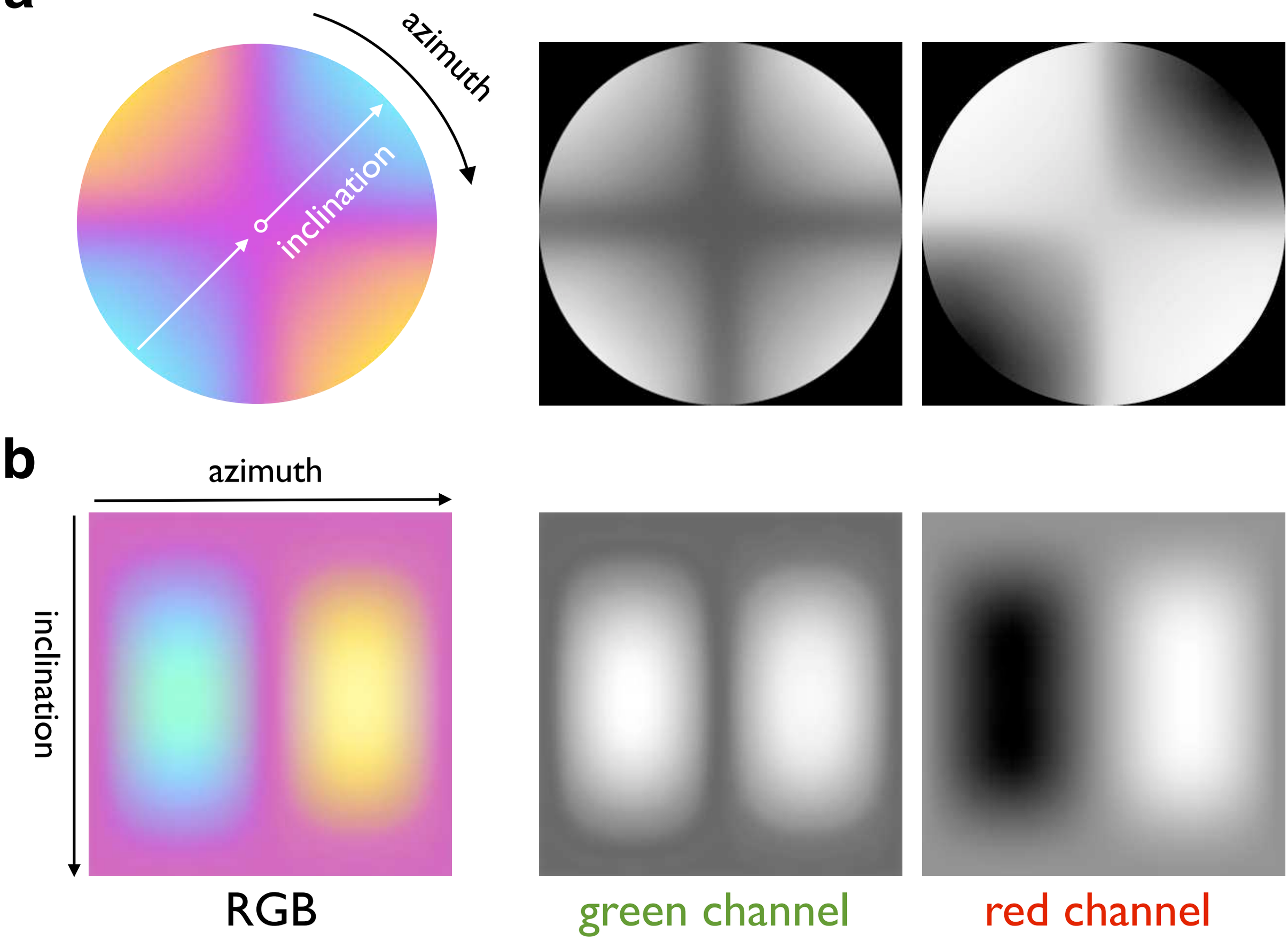

Figure 21.19
Color to monochrome.
(a) Conoscopic image of quartz;
(b) orthogonal projections of (a); coordinate systems as in Figure 21.14.b with inclination extending to 180°.
From left to right: color view (RGB), green channel (500 nm - 600 nm), red channel (600 nm 700 nm).
Note that brightness encoding is used: high intensities are rendered white.

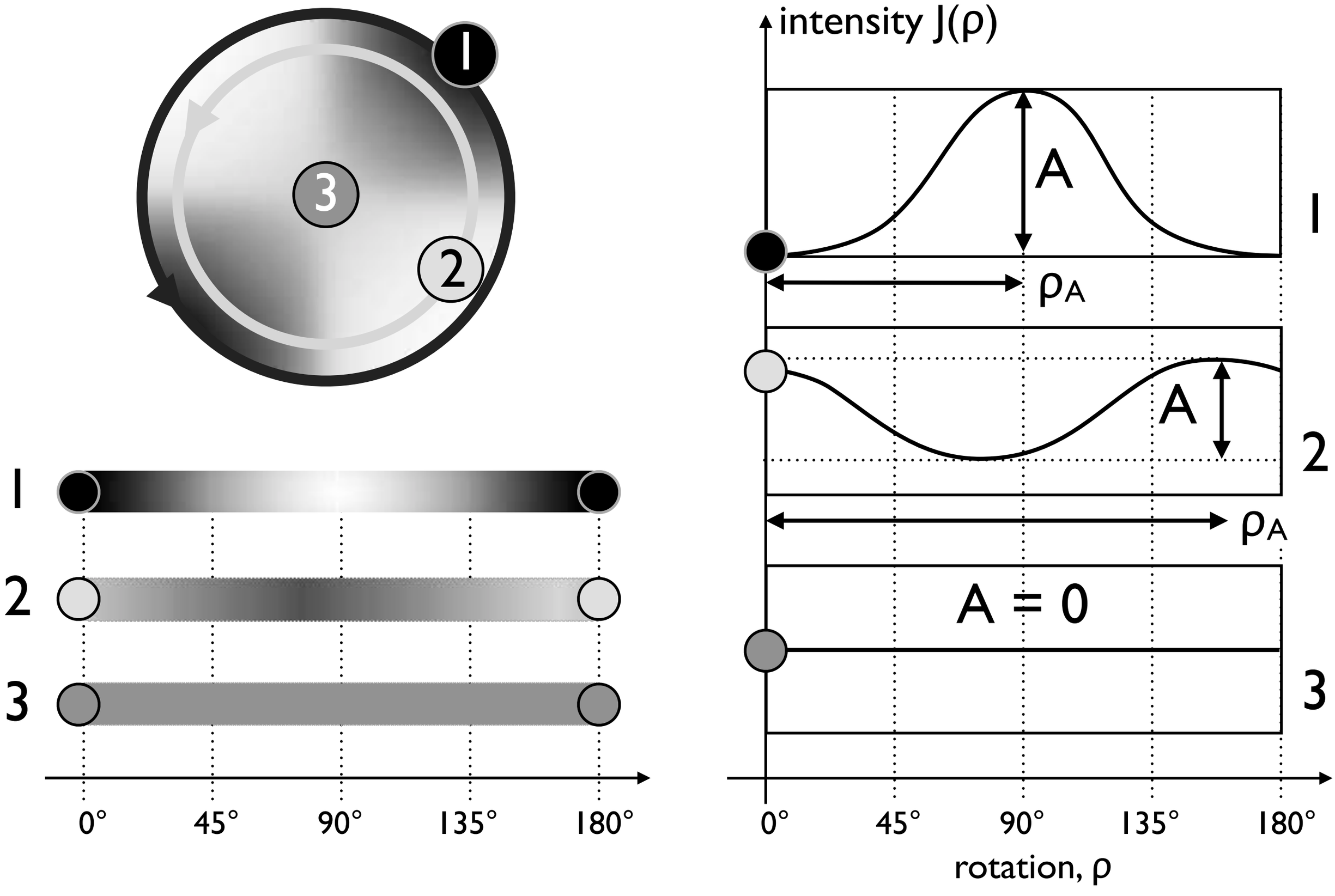

Figure 21.20
Intensity signal of rotating axes.
Rotating the microscope table causes the c-axes to travel in cones about the microscope axis (i.e., in small circles about the center of the conoscopic image).
(a) Conoscopic image showing starting orientation of three grains (1, 2, 3 in Figure 21.2); intensity changes as function of rotation (shown below);
(b) intensity function J(ρ) is characterized by amplitude, A, and phase angle, ρ_A (see Figure 21.3).

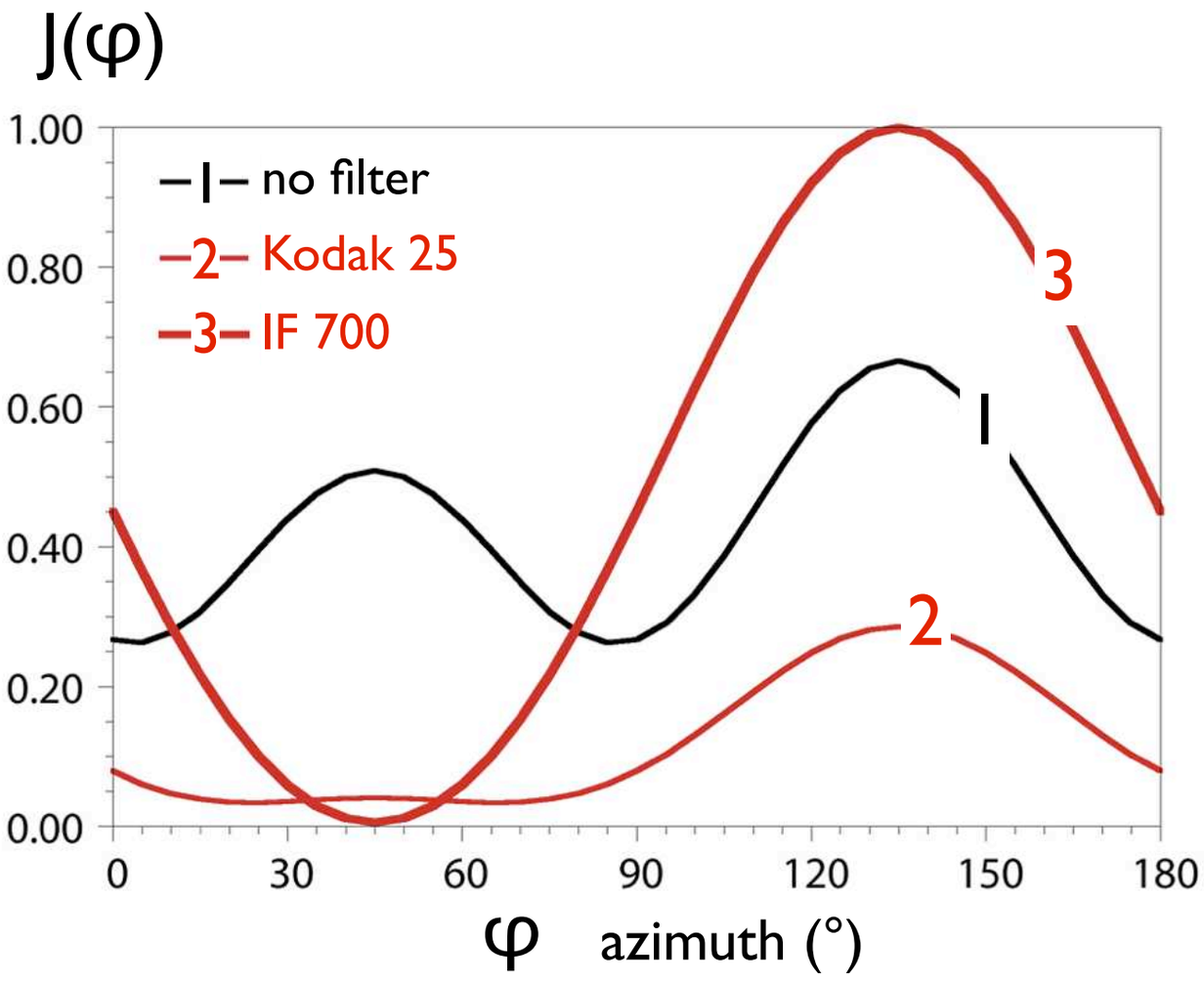

Figure 21.21
Intensity as function of azimuth for different red filters.
Monochrome intensity variations, J(φ) for constant inclination (θ = 90°) using (1) no filter, (2) a Kodak Wratten Filter 25 and (3) a narrow band interference filter, transmitting at 700 ± 5 nm.

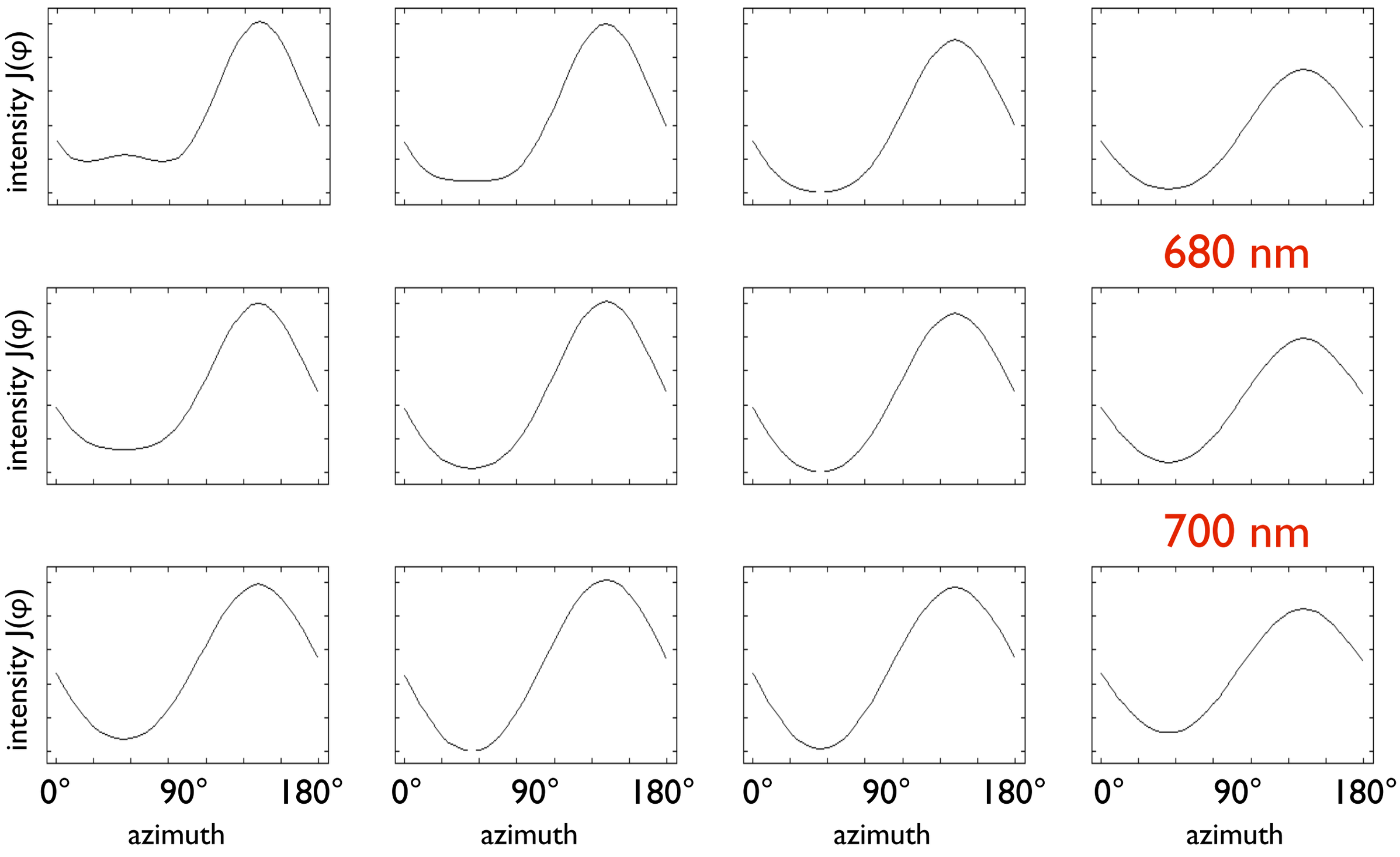

Figure 21.22
Intensity as function of azimuth for red monochrome wavelengths.
Plots of intensity, J(φ), at constant inclination (θ = 90°) are shown for three different wavelengths (λ = 660 nm, 680 nm, and 700 nm) and four different section thicknesses (t = 25 µm, 20 µm, 15 µm, and 10 µm).

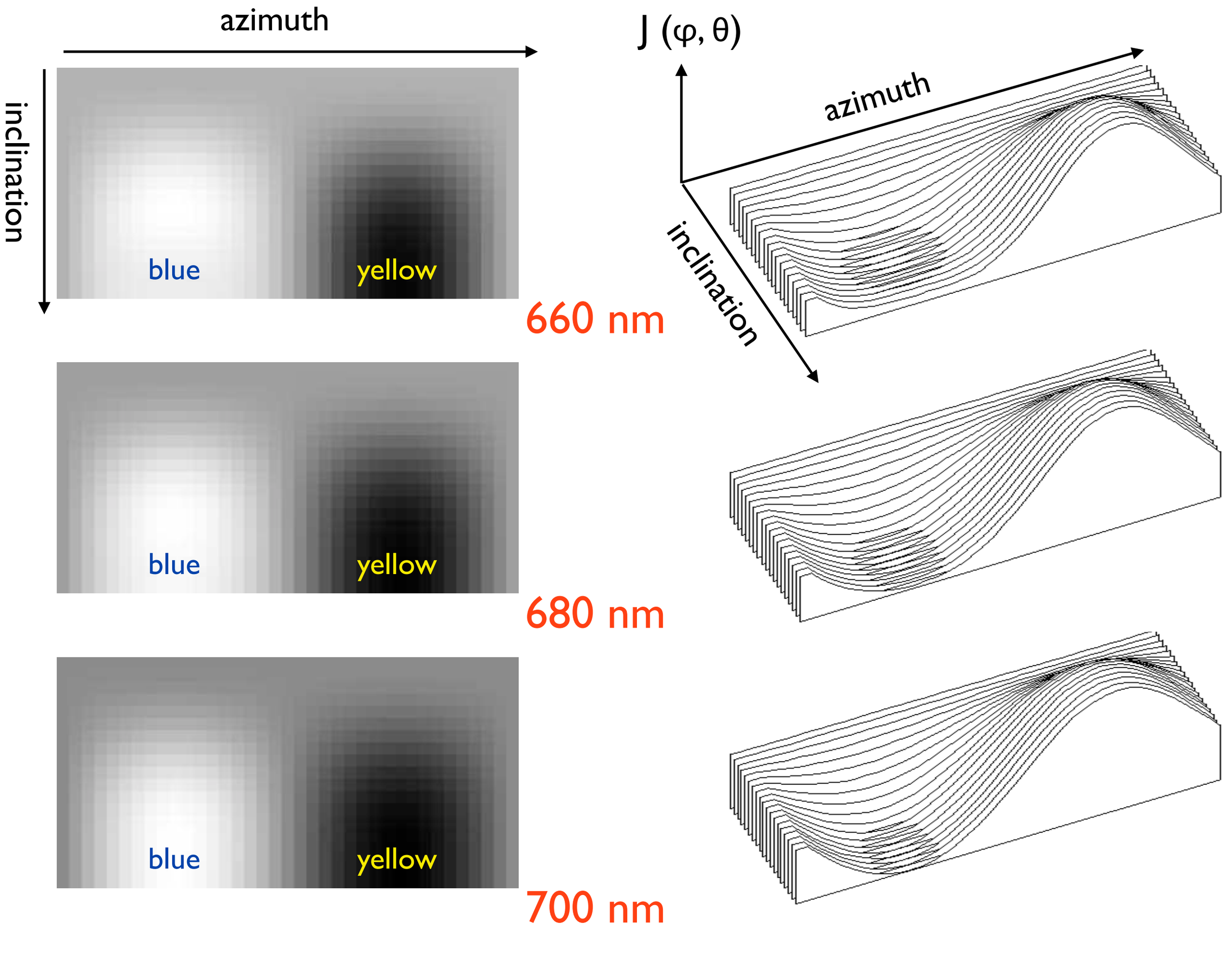

Figure 21.23
Intensity profiles as function of inclination.
Polstack calculated for quartz, 20 μm thickness, crossed polarizers and wave plate inserted; three (φ-θ) slices are shown for λ = 660 nm, 680 nm, and 700 nm; surface plots on the right show 19 J(φ) profiles at 5° increments from θ = 0° (back) to 90° (front).
Note that gray value encoding renders high intensities as black.

a

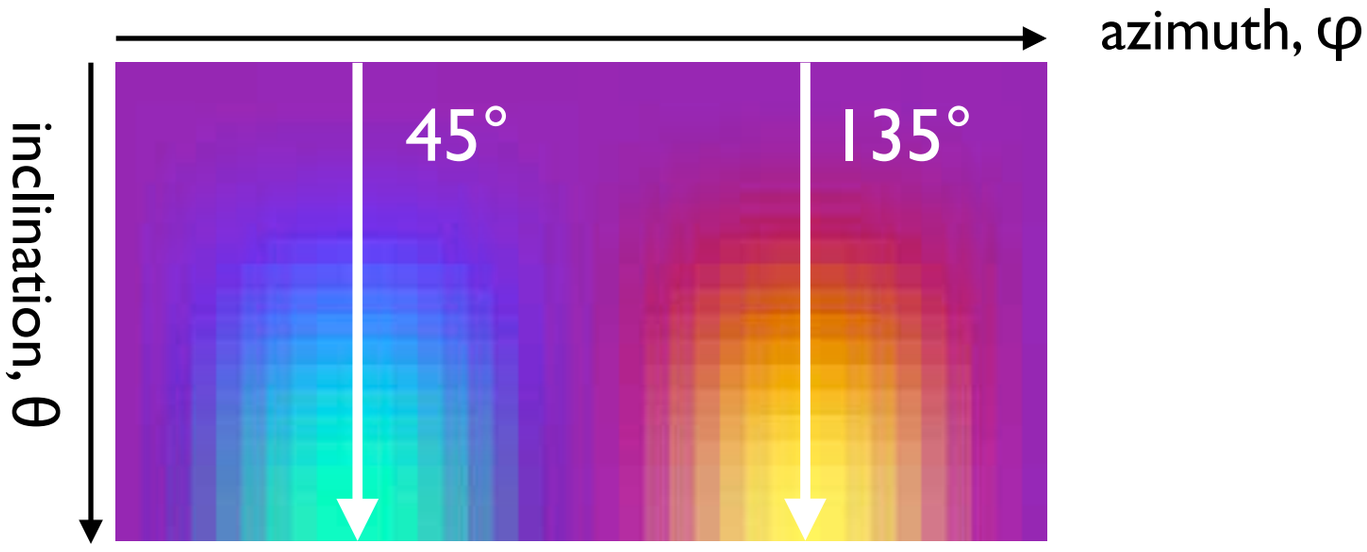
azimuth, φ
inclination, θ
45°
135°

b

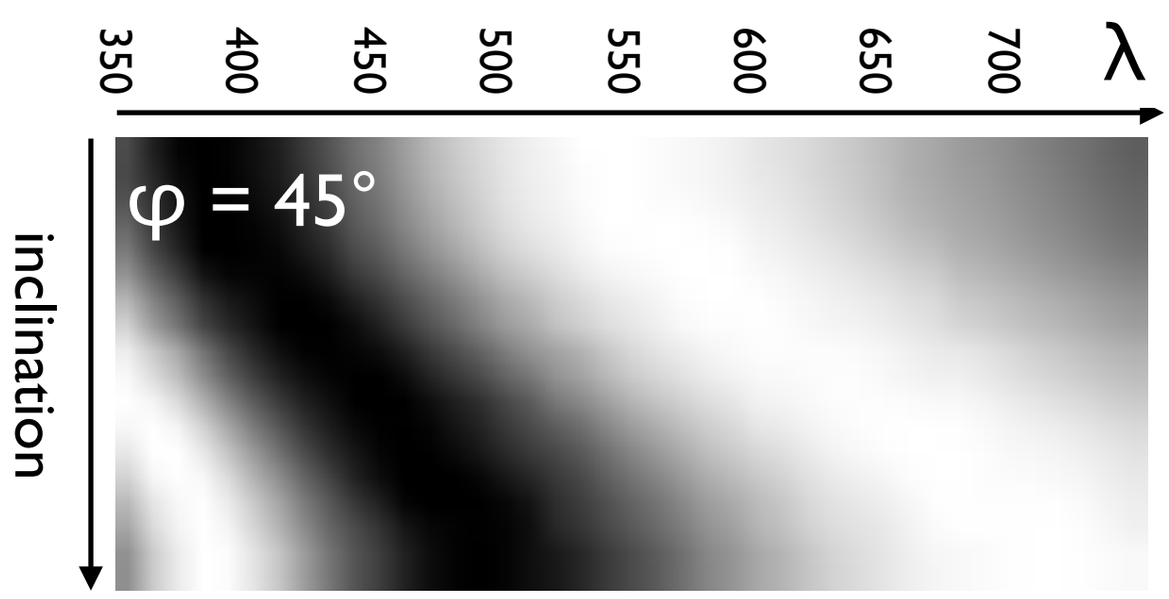
350
400
450
500
550
600
650
700
λ
φ = 45°
inclination

c

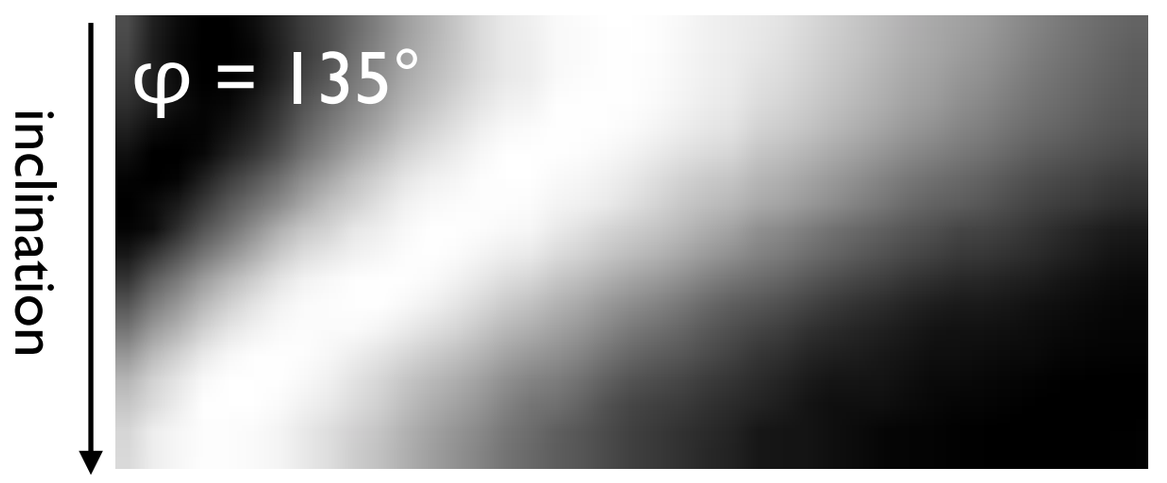
φ = 135°
inclination

d

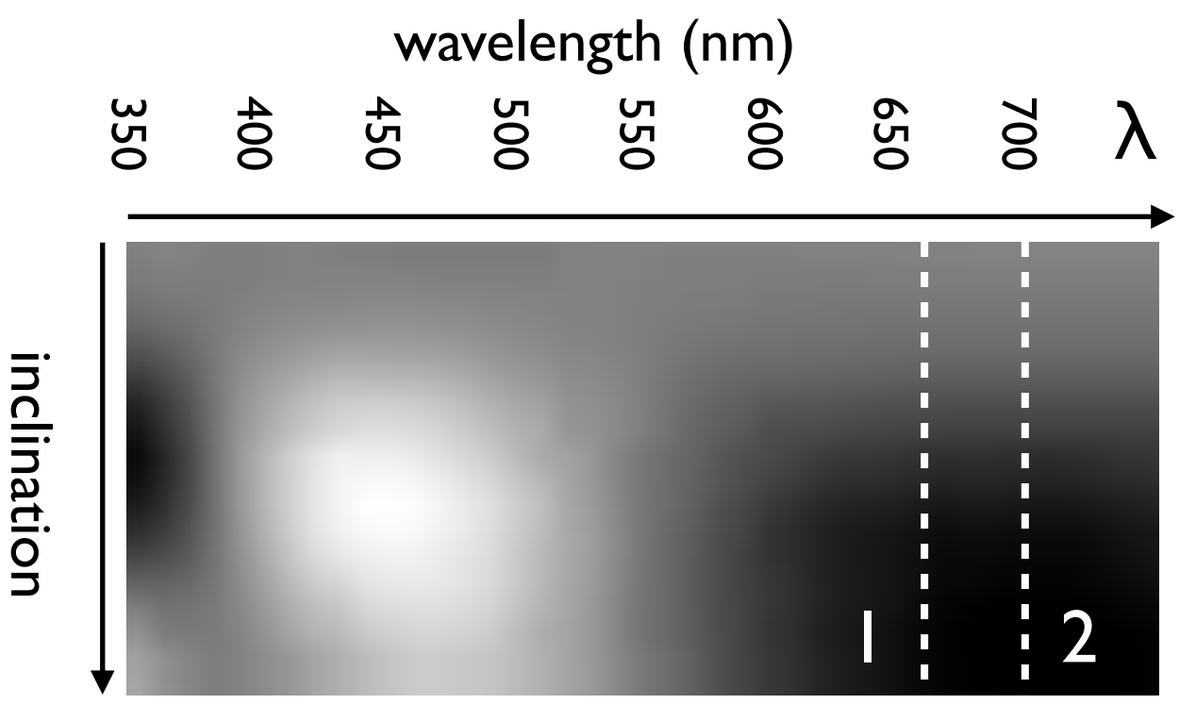
wavelength (nm)
350
400
450
500
550
600
650
700
λ
inclination
I
2

e

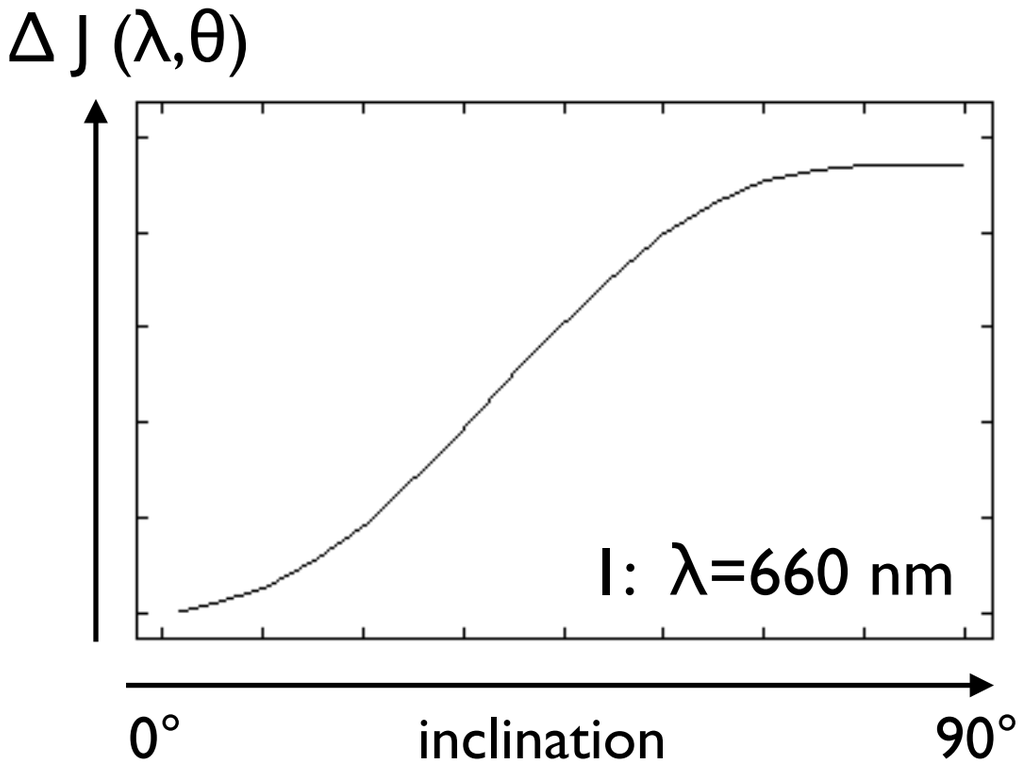
Δ J (λ,θ)
1: λ=660 nm
0°
inclination
90°

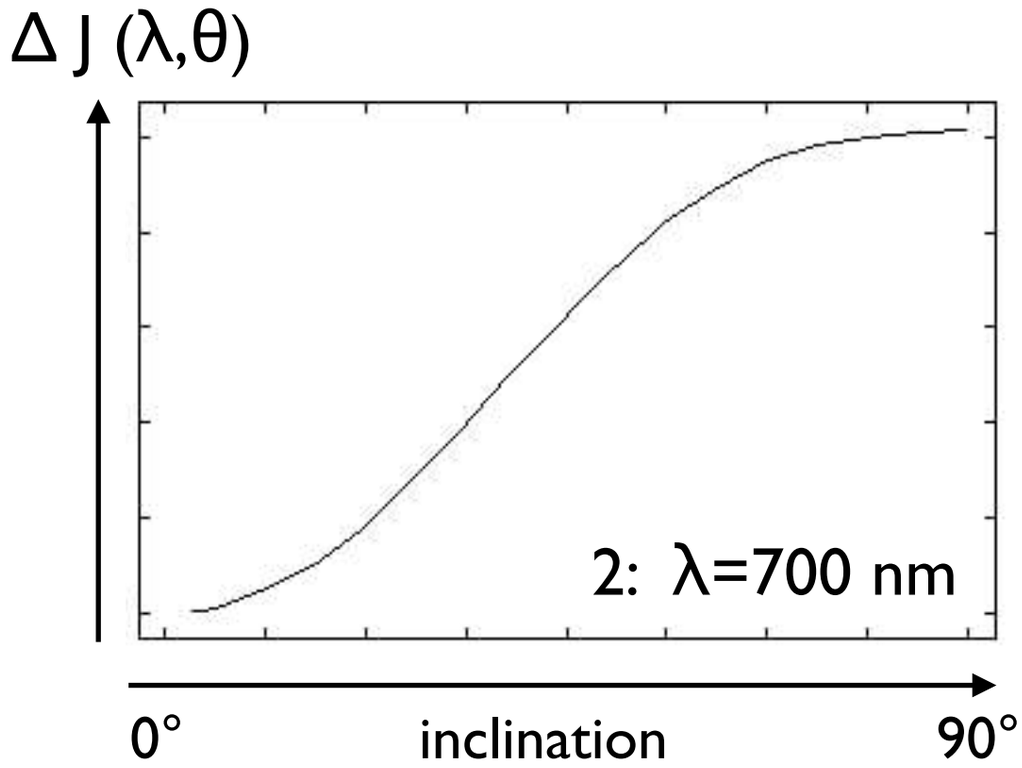
Δ J (λ,θ)
2: λ=700 nm
0°
inclination
90°

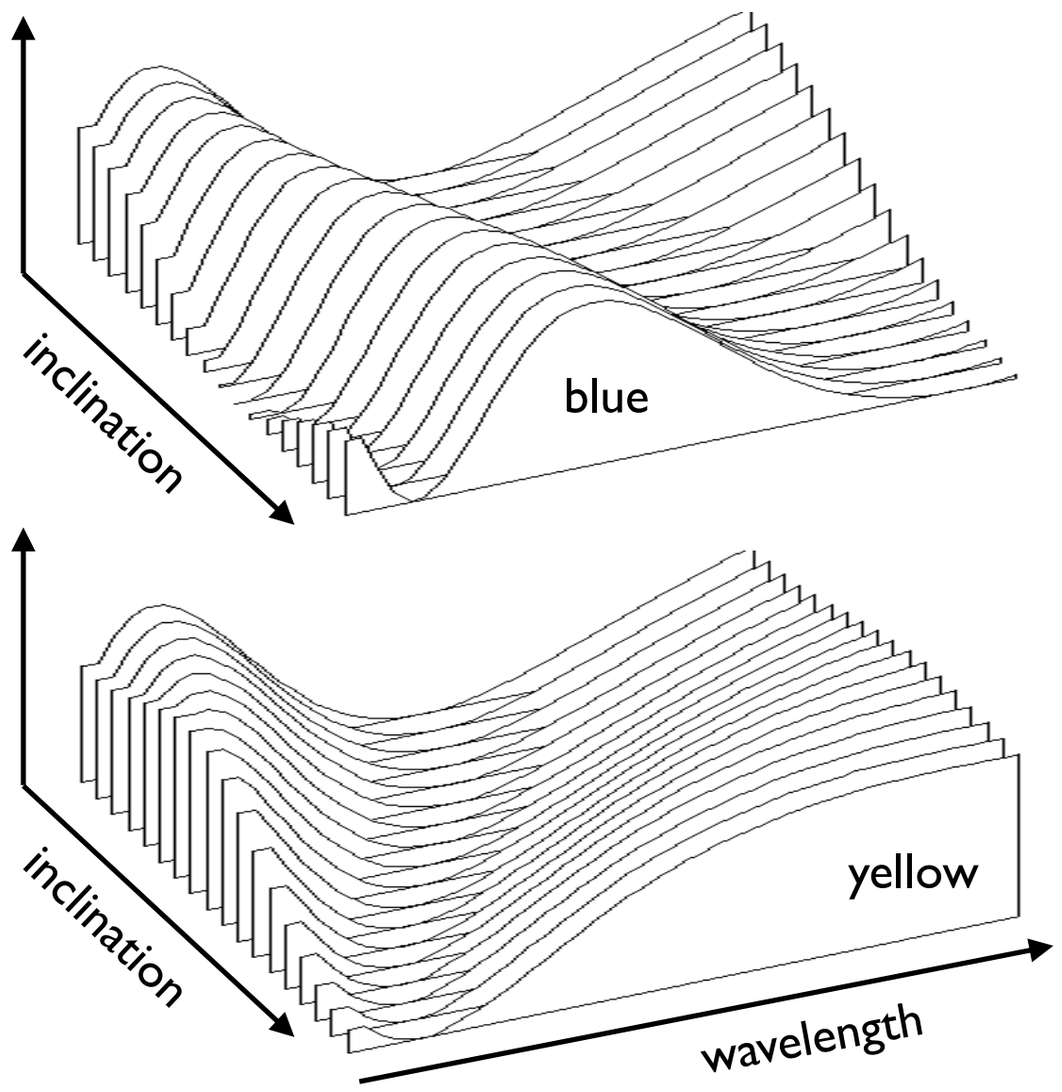
J (λ,θ)
inclination
blue
inclination
yellow
wavelength

Figure 21.24
Amplitude of intensity functions.
Color composite of polstack for quartz section of 20 µm thickness, crossed polarizers, lambda plate inserted; two traces for (θ-λ) sections at two constant azimuth values, φ = 45° (blue) and φ = 135° (yellow) are indicated;
(b) rotated (θ-λ) section of (a) at φ = 45° (blue); on the right, intensity profiles, J(λ), i.e., spectra, for constant inclinations, θ = 0°, 5°, ... 90°;
(c) same as (b) for φ = 135° (yellow).
Note that gray value encoding renders high intensities as black.
(d) difference image (c) - (b); two traces for J(θ) profiles, at λ = 660 nm and λ = 700 nm, are indicated; note that gray value encoding renders high differences as black;
(e) intensity profiles, J(θ), showing blue-yellow intensity difference as recorded at 660 nm and 700 nm. Note better discrimination at high inclinations for 700 nm.

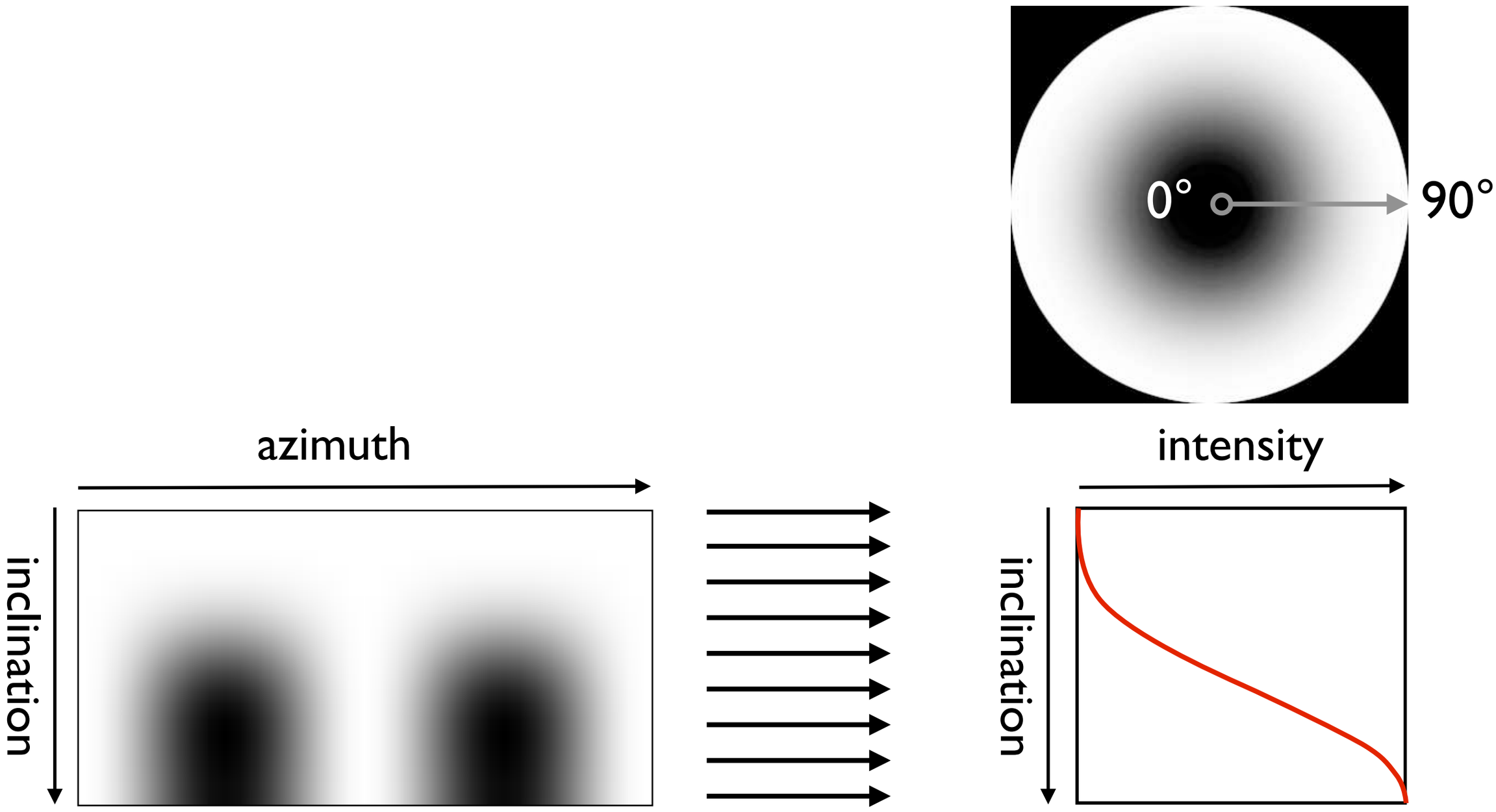

$$\text{integrating} \int_{\varphi = 0°}^{90°} J(\varphi, \theta) = J(\theta)$$

Figure 21.25
Circular polarization.
The intensity, $J(\theta)$, of circular polarization is calculated by summing the intensities $J(\varphi, \theta)$ of the cross polarization over all azimuths, φ. The resulting dependence of intensity on inclination, $J(\theta)$, is shown on the right.
Note that gray value encoding renders high intensities as black.

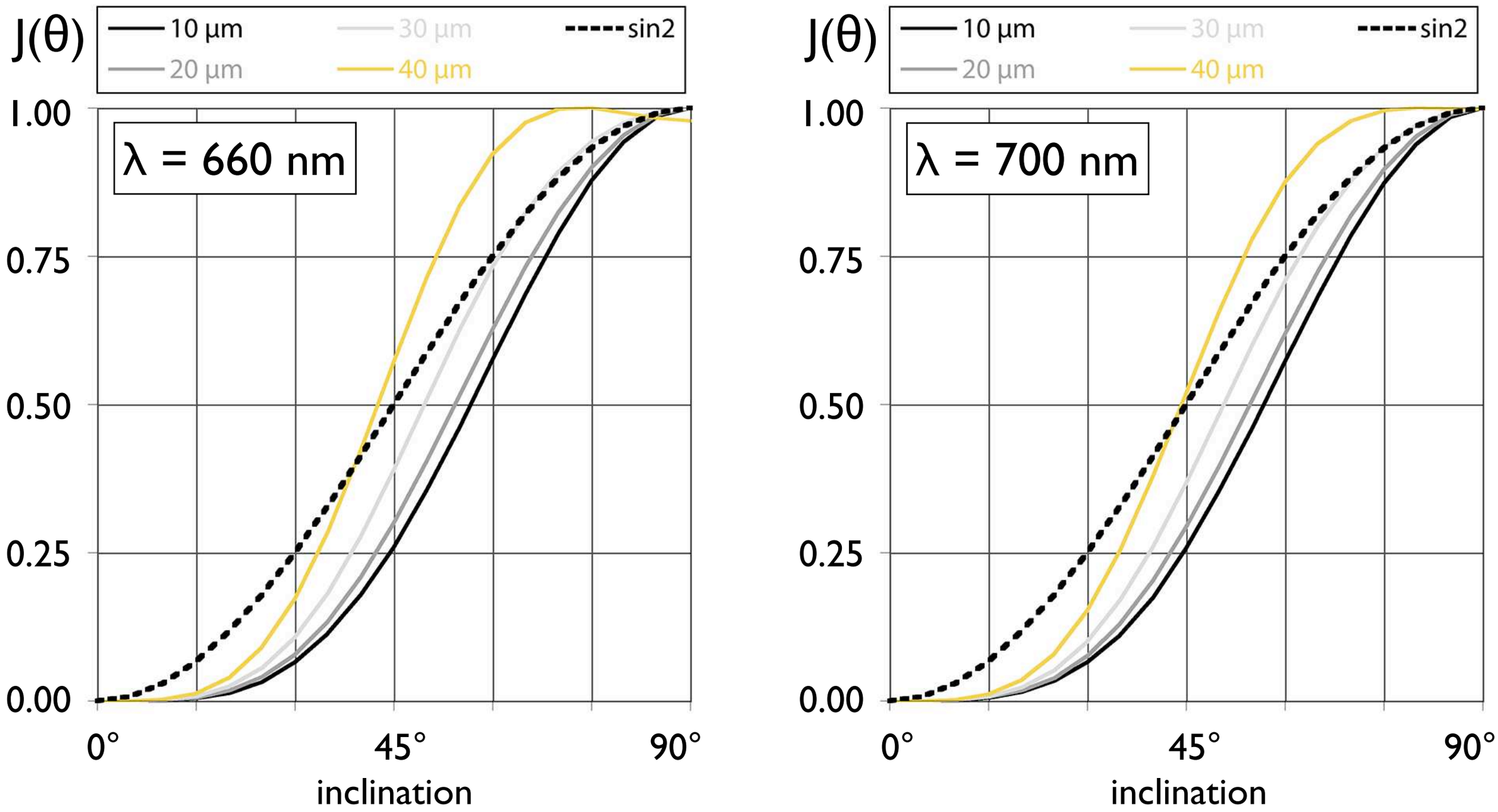

Figure 21.26
The 'sine-square law' of circular polarization.
The dependence of intensity, $J(\theta)$, on inclination is calculated for two different wavelengths, λ = 660 nm and λ = 700 nm, and for four different section thicknesses, from 10 µm to 40 µm; the 'sine-square law', $J = \sin^2(\theta)$, is superposed for comparison.

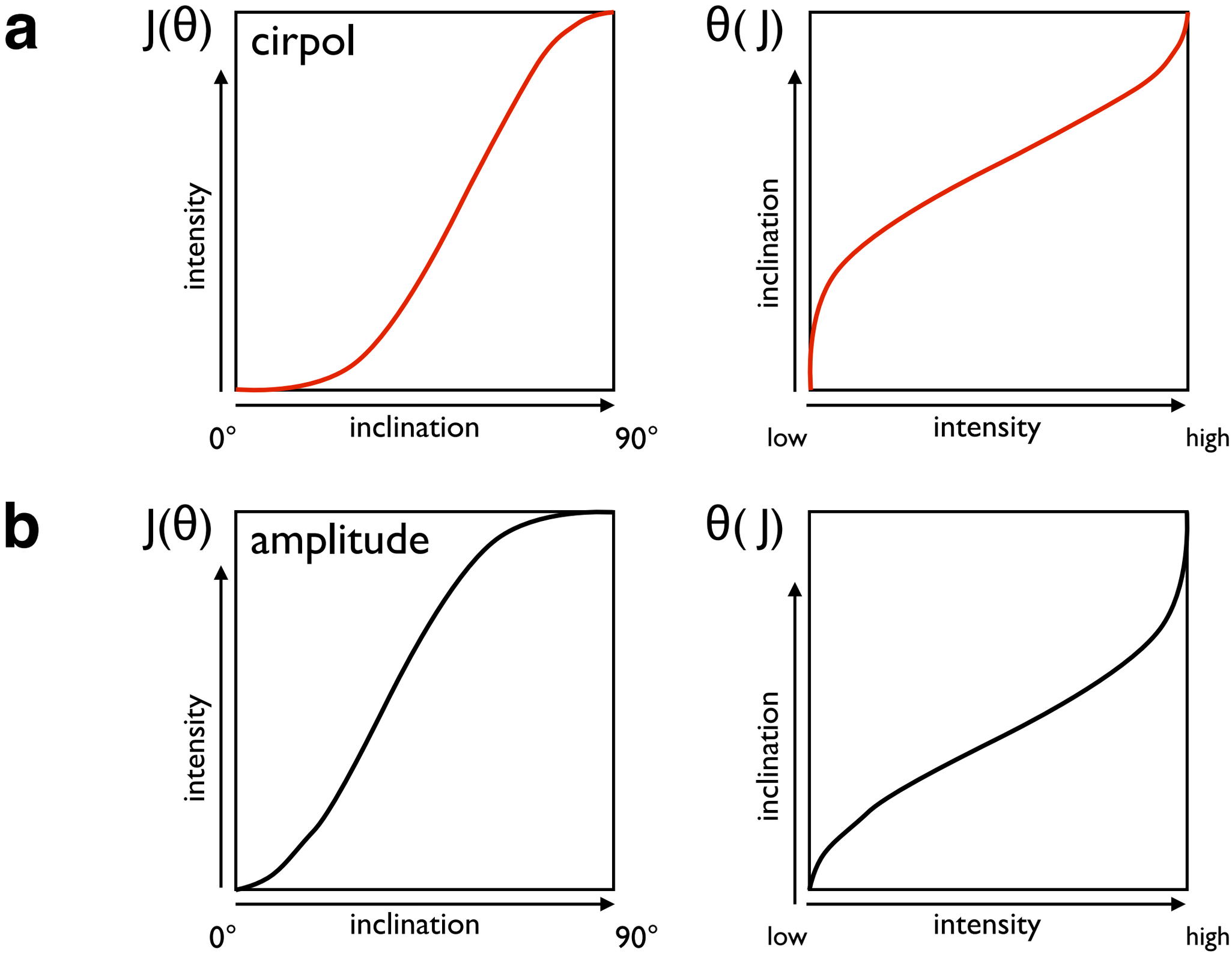

Figure 21.27
Deriving inclinations from intensities.
Two dependencies of intensity on inclination, J(θ), can be used:
(a) J(θ) for circular polarization, t = 20 μm, λ = 700nm (Figure 21.26);
(b) J(θ) derived from difference between first-order blue and first-order yellow ('amplitude') (Figure 21.24.b).
Left: J(θ); right: the inverse function, θ(J); θ(J) serves as look-up table to convert intensities to inclinations.